



eCOMMONS

Loyola University Chicago
Loyola eCommons

Master's Theses

Theses and Dissertations

2017

Dexamethasone Treatment Effects on H3k27me3 Chromatin Organization Is Related to NK Cell Immune Dysregulation

Michael Sarafeno Misale
Loyola University Chicago

Follow this and additional works at: https://ecommons.luc.edu/luc_theses

 Part of the [Immunology and Infectious Disease Commons](#)

Recommended Citation

Misale, Michael Sarafeno, "Dexamethasone Treatment Effects on H3k27me3 Chromatin Organization Is Related to NK Cell Immune Dysregulation" (2017). *Master's Theses*. 3692.
https://ecommons.luc.edu/luc_theses/3692

This Thesis is brought to you for free and open access by the Theses and Dissertations at Loyola eCommons. It has been accepted for inclusion in Master's Theses by an authorized administrator of Loyola eCommons. For more information, please contact ecommons@luc.edu.



This work is licensed under a [Creative Commons Attribution-Noncommercial-No Derivative Works 3.0 License](#).
Copyright © 2017 Michael Sarafeno Misale

LOYOLA UNIVERSITY CHICAGO

DEXAMETHASONE TREATMENT EFFECTS ON H3K27ME3 CHROMATIN
ORGANIZATION IS RELATED TO NK CELL IMMUNE DYSREGULATION

A THESIS SUBMITTED TO
THE FACULTY OF THE GRADUATE SCHOOL
IN CANDIDACY FOR THE DEGREE OF
MASTER OF SCIENCE

PROGRAM IN MICROBIOLOGY AND IMMUNOLOGY

BY

MICHAEL S. MISALE

CHICAGO, ILLINOIS

DECEMBER, 2017

Copyright by Michael S. Misale, 2017
All rights reserved.

ACKNOWLEDGEMENTS

I would like to thank Dr. Herbert Mathews, PhD, for the guidance and support he has provided from the moment I joined the lab and throughout the process of obtaining this degree. Also for being my sounding board for new ideas and experiments presented in this thesis. Additionally, I would like to thank my past and present lab mates, Justin Eddy, Karen Krukowski, Thomas Schenone, Greg Benz, and Sara Knowles, who were always prepared with suggestions and help to assist my work.

I would like to also thank the members of my thesis committee including; Dr. Linda Janusek, and Dr. Susan Baker for their enthusiasm for my work and guidance throughout this process.

Finally, I would like to thank all the members of my family who have encouraged and supported me throughout my time in graduate school. Most of all my parents, without them the prospect of getting an advanced degree would not be possible.

LIST OF TABLES

Table 1. Effect of Dex and NE treatment on IFN gamma production by PBMC and by NK cells	22
Table 2. Nuclear H3K27me3 mean fluorescence intensity (MFI) within dexamethasone (Dex) treated and untreated NK cells	23
Table 3. Localization of H3K27me3 within Dex treated and untreated NK cells	25
Table 4. Relationship between H3K27me3 Modulation and H3K27me3 BDI in untreated and Dex treated NK cell populations from six individuals	28
Table 5. Percentage of Dex and untreated NK cells within H3K27me3 Modulation Intervals with representative localization of H3K27me3	30
Table 6. Relationships between H3K27me3 Modulation and IFN gamma MFI in untreated and Dex treated NK cell populations from six individuals	32
Table 7. Relationship between H3K27me3 BDI and IFN gamma MFI in untreated and Dex treated NK cell populations from six individuals	32
Table 8. H3K27me3 Global Chromatin Organization (CO) Value and Cytoplasmic IFN gamma levels for individual populations of NK cells	37

LIST OF FIGURES

Figure 1. Effect of Dexamethasone (Dex) and Norepinephrine (NE) on NKCA of PBMC	21
Figure 2. Nuclear localization of H3K27me3 in Dex treated and untreated NK cells	25
Figure 3. Relationship of H3K27me3 Modulation to H3K27me3 Bright Detail Intensity (BDI) within NK cells	27
Figure 4. H3K27me3 Modulation and H3K27me3 BDI of Dex treated and untreated NK cells for each H3K27me3 Modulation Interval	28
Figure 5. NK cell Percentage within each H3K27me3 Modulation Interval	31
Figure 6. NK cell H3K27me3 Modulation Interval IFN gamma Production	33
Figure 7. H3K27me3 Modulation Interval Chromatin Organization (CO) of Dex treated and untreated NK cells.	34
Figure 8. Relationship of H3K27me3 Modulation Interval Chromatin Organization (CO) to H3K27me3 Modulation Interval IFN gamma Production in Dex treated and untreated NK cells	35

LIST OF ABBREVIATIONS

Dex	Dexamethasone
NE	Norepinephrine
PBMC	peripheral blood mononuclear cells
NK	natural killer
NKCA	natural killer cytolytic activity
DPM	disintegrations per minute
GC	glucocorticoid
GR	glucocorticoid receptor
GRE	glucocorticoid response element
nGRE	negative glucocorticoid response element
H3K9ac	histone-3 lysine-9 acetylation
H3K27me3	histone-3 lysine-27 tri-methylation
MFI	mean fluorescence intensity
BDI	bright detail intensity
CO	chromatin organization
HPA	hypothalamus-pituitary- adrenal
SNS	sympathetic nervous system
PBS	phosphate buffered saline
BSA	bovine serum albumin
IFN gamma	interferon gamma

NPC	nuclear pore complex
TADs	topological associated domains
EZH	enhancer of zeste homologue
PRC	polycomb repressive complex
HDAC	histone deacetylase
MHC	major histocompatibility complex
H3	histone-3
H4	histone-4
CRH	corticotropin releasing hormone
ATCH	adrenocorticotropic hormone
B2-AR	beta-2 adrenergic receptor
AC	adenylate cyclase
cAMP	cyclic adenosine-5 monophosphate
HSP	heat shock protein

TABLE OF CONTENTS

ACKNOWLEDGEMENTS	iii
LIST OF TABLES	iv
LIST OF FIGURES	v
LIST OF ABBREVIATIONS	vi
ABSTRACT	x
CHAPTER ONE: INTRODUCTION	
Literature Review	1
The Stress Response	1
The Stress Response's Effects on Immune System	2
NK Cell Function and the Immune System	2
NK Cell Function and Stress Hormones	4
NE: B2-AR Signaling	4
GC: GR Signaling	5
Epigenetics and Chromatin Organization	7
GC: GR Signaling and Chromatin Organization	8
Aims and Hypotheses	10
Significance	11
CHAPTER TWO: METHODS AND MATERIALS	12
Cell Lines and Media	12
Subject Recruitment	12
<i>In vitro</i> Cellular Treatment of Human PBMC	12
Natural Killer Cell Activity (NKCA)	13
Measurement of IFN gamma by ELISA	14
Intracellular Staining of Human PBMC	14
IDEAS Software Analysis of H3K27me3 in PBMC	15
Automation of H3K27me3 Localization with IDEAS Software	15
Confirmation that H3K27me3 Modulation and H3K27me3 Bright Detail Intensity (BDI)	
Differentiate Peripheral and Non-Peripheral H3K27me3 Localization in NK Cell Nuclei	16
IDEAS Analysis of H3K27me3 Modulation Interval IFN gamma Production in NK cells	17
Calculation of H3K27me3 Modulation Interval Chromatin Organization	18
Calculation of H3K27me3 Global CO and Global IFN gamma Production	18

Statistical Analyses	19
CHAPTER THREE: RESULTS	20
Effects of Dexamethasone (Dex) and Norepinephrine (NE) on PBMC NKCA	20
Effects of Dex and NE on IFN gamma production by PBMC and CD3 ⁺ CD56 ⁺ NK Cells	21
Effects of Dex on H3K27me3 Levels in NK Cells	23
Localization of H3K27me3 within Dex Treated NK Cells	24
Localization and Density Quantification of NK Cell Nuclear H3K27me3	26
Relationships of H3K27me3 Modulation and H3K27me3 BDI to Cytoplasmic IFN gamma Levels in NK Cells	31
H3K27me3 Modulation Interval Chromatin Organization (CO) of Dex Treated and Untreated NK Cells	33
H3K27me3 Global Chromatin Organization (CO) of Dex Treated and Untreated NK Cells with regard to NK Cell IFN gamma Production	36
CHAPTER FOUR: DISCUSSION	38
BIBLIOGRAPHY	47
VITA	62

ABSTRACT

It is well-established that psychological stress reduces natural killer (NK) cell immune function. This reduction is mediated by stress-induced release of glucocorticoids (GC), which can suppress immune function. Associated with suppression of a particular immune function are GC induced histone-epigenetic marks. Histone-epigenetic marks are responsible for the organization and compartmentalization of genomes into transcriptionally active euchromatin domains that are localized to the interior of the nucleus. Transcriptionally silent heterochromatic domains are enriched with methylated epigenetic marks and are localized to the nuclear periphery. The purpose of this investigation was to assess the influence of GC on H3K27me3 chromatin organization by measurement of that repressive epigenetic mark. As well as the relationship of H3K27me3 chromatin organization to NK cell effector function, i.e. interferon (IFN) gamma production, was determined. IFN gamma was selected because it is the prototypic cytokine produced by NK cells and is known to modulate both innate and adaptive immunity. GC treatment of human peripheral blood mononuclear cells significantly reduced IFN gamma production. GC treatment produced a distinct NK cell H3K27me3 chromatin organization phenotype. This phenotype was localization of the histone post-translational epigenetic mark, H3K27me3, to the nuclear periphery and was directly related to the reduced production of IFN gamma by NK cells. This nuclear phenotype was determined by direct visual inspection and by use of an automated, high through-put technology, the Amnis ImageStream. This technology combines the per-cell information content provided by standard microscopy with the statistical significance afforded by large sample sizes common to standard flow cytometry. Most

importantly, this technology provided for direct assessment of the localization of H3K27me3 within individual nuclei. These results demonstrate GC to reduce NK cell function at least in part through altered H3K27me3 nuclear organization and suggests that H3K27me3 chromatin organization may be a predictive measure of GC induced immune dysregulation in NK cells.

CHAPTER ONE

INTRODUCTION

Literature Review

The Stress Response.

Psychological stress results in the activation of the hypothalamic pituitary adrenal (HPA) axis as well as the sympathetic nervous system (SNS) (Firdaus S. Dhabhar & McEwen, 1997; F. S. Dhabhar, Miller, McEwen, & Spencer, 1995; F. S. Dhabhar, Miller, Stein, McEwen, & Spencer, 1994). Upon activation of the HPA axis corticotropin releasing hormone (CRH) is released from the hypothalamus (Bernardini et al., 1994); CRH then activates the release of adrenocorticotrophic hormone (ACTH) from the anterior pituitary (Whitnall, 1993) which then regulates the release of glucocorticoids (i.e. cortisol) from the adrenal cortex. Psychological stressors also activate the SNS that culminates in the release of catecholamines (epinephrine and norepinephrine) into the circulation. Epinephrine is released from the adrenal medulla, while norepinephrine (NE) is released from sympathetic nerves that directly innervate host tissues including secondary lymphoid tissues (Madden, Felten, Felten, & Bellinger, 1995). There is a bi-directional, positive feedback loop between the HPA axis and the SNS (Elenkov, Wilder, Chrousos, & Vizi, 2000). In mouse models, centrally administered CRH activated the SNS to produce catecholamines (Irwin, Hauger, & Brown, 1992). Further, NE release from sympathetic neurons (Ma & Morilak, 2005) that directly innervate the hypothalamus or electrical neuronal stimulation (Hosoi, Okuma, & Nomura, 2000) also facilitated activation of the HPA axis. Therefore, activation of one pathway leads to the activation of the other.

The Stress Response's Effect on the Immune System.

Studies in humans and in animals demonstrate that the immune system is influenced by psychological stress (Glaser & Kiecolt-Glaser, 2005; Kusnecov & Rabin, 1994; Segerstrom & Miller, 2004). Psychological stress is also associated with an increased risk for disease, which suggests a linkage among stress, the risk for disease, and the immune system (Glaser & Kiecolt-Glaser, 2005; Segerstrom & Miller, 2004). Cytokine production by the immune system, including IFN gamma, is particularly sensitive to stress dysregulation (Connor, Brewer, Kelly, & Harkin, 2005; Curtin, Boyle, Mills, & Connor, 2009; Curtin, Mills, & Connor, 2009; Goujon et al., 1995; Meltzer et al., 2004), such dysregulation is a likely contributor to stress-related disease susceptibility. HPA axis activation resulting in increased circulating levels of glucocorticoids (GC) (Connor, Kelly, & Leonard, 1997; Laugero & Moberg, 2000; Shanks, Griffiths, Zalcman, Zacharko, & Anisman, 1990; Sheridan et al., 1991) are known to dysregulate immune function. Similarly, SNS activation culminating in the release of NE has also been demonstrated to dysregulate immune function. (Madden, Sanders, & Felten, 1995; Rosenne et al., 2014; Takamoto et al., 1991; Whalen & Bankhurst, 1990).

NK Cell Function and the Immune System.

NK cells belong to the family of group 1 innate lymphocytes (ILC1), their frequency approximates 10% in peripheral blood, and are functionally characterized by their cytotoxicity and their ability to produce cytokines (Vivier, Tomasello, Baratin, Walzer, & Ugolini, 2008). Mature NK cells are poised to secrete cytokines and chemokines that shape the innate and adaptive immune responses (Vivier et al., 2011). However, the best-characterized cytokine produced by NK cells is IFN gamma (Cooper et al., 2001), which is quickly released within minutes to hours after NK cell stimulation (Stetson et al., 2003). NK cell produced IFN gamma

has many effects on the immune response, including induction of MHC class II molecules on antigen-presenting cells, activation of myeloid cells and induction of T helper 1 (TH1) cells (Morvan & Lanier, 2016). Macrophage activation by NK cell-derived IFN gamma has been shown to be essential for resistance to primary tumorigenesis (O'Sullivan et al., 2012) as well as activate killing of obligate intracellular pathogens (Filipe-Santos et al., 2006). In patients and animal models, impaired NK cells or NK cell deficiency have been associated not only with recurring virus infections, but also with an increased incidence of various types of cancer (Orange, 2013). Additionally, human studies of complete NK cell deficiency resulted in the occurrence of fatal infections during childhood (Orange, 2006). NK cells are able to recognize and then spontaneously kill 'stressed' cells, such as infected or tumor cells, without prior sensitization.

As opposed to other immune cells that require a considerable length of time to acquire cytolytic activity, NK cells are 'ready for effector function', which provides a powerful tool for host protection. Numerous studies have demonstrated decreased NK cell function in cancer patients (Nakajima, Mizushima, Nakamura, & Kanai, 1986; Pross & Lotzová, 1993; Schantz, Shillitoe, Brown, & Campbell, 1986) or their families (Hersey, Edwards, Honeyman, & McCarthy, 1979; Strayer, Carter, & Brodsky, 1986), including a long-term epidemiological study reporting that subjects with low NK cell activity had a higher risk of developing various types of cancer (Imai, Matsuyama, Miyake, Suga, & Nakachi, 2000). NK cell deficiencies, characterized by the absence of NK cells or NK cell function (Spinner et al., 2014) lead to higher rates of malignancy. As such, IFN gamma production by NK cells is central to the optimal function of the immune system including innate and adaptive immunity. Measurement of its production in

NK cells is particularly important because the response to stimulus is essentially immediate and does not require longer term activation as would be required with T lymphocytes.

NK Cells and Stress Hormones.

NK cells have been demonstrated to be susceptible to the effects of both NE and GC treatment. All lymphoid cells express beta-2 adrenergic receptors (B2-AR) with the exception of CD4 T helper 2 cells (Sanders et al., 1997). NK cells, CD8 T cells, and CD4 helper 1 T cells respond to NE through expression of the B2-AR receptor on their cell surface. (Maisel, Harris, Rearden, & Michel, 1990). NK cells have the highest expression of B2-AR of any of the immune cell subsets and have been shown to be incredibly responsive to NE treatment (Khan, Sansoni, Silverman, Engleman, & Melmon, 1986). NE has been demonstrated to decrease NK cell IFN gamma production and NKCA (Rosenne et al., 2014; Takamoto et al., 1991; Whalen & Bankhurst, 1990) through a B2-AR dependent pathway (described below). While the glucocorticoid receptor (GR), that responds to GC, is ubiquitously expressed in all cell types and has been demonstrated to reduce NKCA and IFN gamma production by NK cells through both genomic and non-genomic mechanisms (described below). Therefore, NK cells are extremely responsive to stress hormones resulting from activation of both the HPA axis and the SNS, and serve as a model system to understand how stress hormones modulate immune function.

NE and B2-AR.

NE transduce their signal through the stimulation of B2-AR. B2-AR activation then directly activates G-coupled proteins that stimulate adenylate cyclase (AC). Stimulated AC then induces the production of the second messenger cyclic adenosine-5' monophosphate (cAMP) within the cell (Kitakaze et al., 1991). Increased cAMP levels are known to inhibit NF-kB, AP-1, and NF-AT activation, which are transcription factors required for the production of

inflammatory cytokines like IFN gamma (Haraguchi, Good, & Day, 1995; Haraguchi, Good, James-Yarish, Cianciolo, & Day, 1995a, 1995b; Panina-Bordignon et al., 1997; Parry & Mackman, 1997) and modulate cytotoxicity of NK cells (Krzewski, Gil-Krzewska, Nguyen, Peruzzi, & Coligan, 2013; Zhou, Zhang, Lichtenheld, & Meadows, 2002).

GC: GR Signaling.

Cortisol, the most abundant glucocorticoid in humans, is produced by the adrenal gland and is transported through the blood bound to corticosteroid-binding globulin (CBG) and albumin (Torpy & Ho, 2007). Cortisol is a lipophilic ligand that passively diffuses through the cell membrane into the cytoplasm, where it binds to and activates its cognate receptor GR (Nicolaidis, Galata, Kino, Chrousos, & Charmandari, 2010). In the un-activated state, GR exists predominantly within the cytoplasm and is bound to a multimeric molecular chaperone complex, which includes heat shock proteins (HSPs) 90, 70, and 50, and immunophilins. HSP90 regulates ligand binding, retains GR in the cytoplasm, and masks GR's two nuclear localization sequences. Upon binding GC, GR undergoes conformational changes that releases it from chaperone proteins and activating GR to modulate NK cell function through genomic and non-genomic mechanisms (Beck et al., 2009).

GC effects at the non-genomic level are by GC: GR interactions at the cell membrane or within the cytoplasm. GC: GR non-genomic actions are rapid, typically within minutes and are in contrast to the genomic, which require hours or days for effect (Ayroldi et al., 2012; Groeneweg, Karst, de Kloet, & Joëls, 2011). The non-genomic effects of GC do not require *de novo* protein synthesis (Oakley & Cidlowski, 2013), and result from GC:GR direct interactions with membrane proteins (e.g., G-protein-coupled receptors, ion channels, and T cell receptors), (Löwenberg, Verhaar, van den Brink, & Hommes, 2007; Stahn & Buttgerit, 2008; Stahn,

Löwenberg, Hommes, & Buttgereit, 2007) or occur within the cytosol by direct interaction with kinases (e.g. extracellular signal-regulated kinases, c-Jun NH₂-terminal kinases, and the p38 isoforms) thus impacting signal transduction pathways (Ayroldi et al., 2012). At the non-genomic level, GC:GR can destabilize mRNA, interfere with transcription factor access to the nucleus (Almawi & Melemedjian, 2002; Barnes, 2010; Flammer & Rogatsky, 2011; Reily, Pantoja, Hu, Chinenov, & Rogatsky, 2006), alter the physicochemical properties of plasma and mitochondrial membranes (Falkenstein, Tillmann, Christ, Feuring, & Wehling, 2000; Löwenberg et al., 2007), and modify the composition (Van Laethem et al., 2003), or the formation (Yamagata et al., 2012) of lipid rafts.

At the genomic level, GC:GR do not bind to DNA in a stable manner, but shuttle between the nucleoplasm and GC-responsive elements (GRE) located in the promoter or enhancer regions of GC-responsive genes (Bush, Krukowski, Eddy, Janusek, & Mathews, 2012; McNally, Müller, Walker, Wolford, & Hager, 2000; Voss et al., 2011). Within the nucleus target gene transcription is either enhanced or repressed by several GR dependent mechanisms based on the context of the GR genomic interaction. These mechanisms include direct binding of GR to specific *cis*-acting GRE DNA sequences. GR binding to GRE typically leads to enhanced gene transcription of GC induced target genes. Less often, GRE occupancy can repress gene transcription (Uhlenhaut et al., 2013) GR can also repress genes by tethering itself to other transcription factors repressing their capacity to induce gene transcription (De Bosscher, Vanden Berghe, & Haegeman, 2000; De Bosscher, Vanden Berghe, Vermeulen, et al., 2000). GR also binds to inverted palindromic sequences known as negative GREs (nGREs) (So, Chaivorapol, Bolton, Li, & Yamamoto, 2007) which also inhibit transcription of target genes. GR recruitment to nGREs promotes the assembly of corepressor complexes and the recruitment of histone deacetylases, which direct

glucocorticoid-dependent repression of specific genes by compaction of chromatin through deacetylation of lysines on histone H3 or H4 (Surjit et al., 2011). In direct contrast, GR homodimers can also interact with GRE and stimulate potent gene expression through transactivation (Abraham et al., 2006; Bhattacharyya, Zhao, Kay, & Muglia, 2011; D'Adamio et al., 1997; Zhao et al., 2006). GR recruitment of co-activators like CREB-binding protein (CBP), P300/CBP-associated factor (pCAF), or steroid receptor coactivators (SRCs), confer local histone acetyltransferase activity, resulting in the local acetylation of lysines on H3 or H4, decondensing chromatin and increasing access for relevant transcription factors, resulting in marked gene transcription (Barnes, 2006; X. Li, Wong, Tsai, Tsai, & O'Malley, 2003).

Epigenetics and Chromatin Organization.

Epigenetics refers to a heritable change in a phenotype that does not involve changes in the DNA sequence, including histone post-translational modifications. The deposition of histone post-translational modifications can result in heritable changes in gene expression or in stable, long-term alterations of the transcriptional potential of the cell, which may not be heritable. DNA is wrapped around an octomeric protein complex, consisting of two of each of the histone proteins (H2A, H2B, H3, and H4). The combination of 146 bps of DNA and histone proteins composes the nucleosome which is the basic unit of chromatin. Histone acetylation and histone methylation are the most-characterized epigenetic marks. Acetylation and methylation of histones are responsible for the compartmentalization of the genomes into distinct domains, transcriptionally active euchromatin, and transcriptionally silent heterochromatin (Martin & Zhang, 2005; Misteli, 2007). Acetyl groups are added to lysine residues, neutralizing their positive charge, disrupting the interaction with DNA's negative charge, and loosening the compaction of chromatin. Relaxing the chromatin structure increases its accessibility to

transcription factors and, subsequently, gene expression. Removal of acetyl groups results in condensation of chromatin, repressing gene expression (Cosgrove & Wolberger, 2005).

Condensed heterochromatin is enriched in tri-methylation of H3K9 and H3K27, and silencing of euchromatin by histone deacetylases involves the recruitment of specific lysine histone methyltransferases (Kouzarides, 2007). Unlike histone acetylation, histone methylation does not affect the negative charge of DNA, but represses transcription through the recruitment of co-repressors such as retinoblastoma protein pRb, KAP1, or polycomb repressive complex 1 and 2 (PRC1, PRC2)(Margueron & Reinberg, 2011; Nielsen et al., 2001; Simon & Kingston, 2009).

In addition to regulating gene transcription, epigenetic marks have also been shown to localize chromatin to discrete areas within cell nuclei. Euchromatin enriched for acetylated epigenetic marks tend to localize in the interior of the nucleus, while heterochromatic chromatin enriched with histone methylation marks tend to localize toward the nuclear periphery (Andrulis, Neiman, Zappulla, & Sternglanz, 1998; Williams et al., 2006; Zink, Fischer, & Nickerson, 2004). The nuclear localization of histone methylation marks in three-dimensional preserved nuclei identified peripheral localization of methylated marks in colon carcinoma and breast carcinoma cell lines (Cremer et al., 2004). Taken together, these observations indicate that histone epigenetic marks influences chromatin organization by affecting contacts between different histones and between histones and DNA.

GC: GR and Chromatin Organization.

At the global-genomic level GR interacts with thousands of sites across the genome, influencing the expression of hundreds of genes (Reddy et al., 2009; So et al., 2007; Wang et al., 2004). These GR binding sites potentiate clusters of transcription factor binding across the entire genome with interactions between distal sites that dramatically alter their regulatory activities

(Vockley et al., 2016). At this scale, the effect of GC are coordinated transcriptionally through alterations in chromatin organization. Alterations in chromatin organization determine which genes are repressed and which genes are transcribed. By genome-scale chromosome conformation capture, chromatin has been demonstrated to be organized into large compartments that are “open” and highly transcribed or “closed” and less transcriptionally active (Lieberman-Aiden et al., 2009). Compartments are comprised of topologically-associated chromosomal domains (TADs, containing DNA segments ranging in length from hundreds of kilobases to many megabases (Dixon et al., 2012; Gibcus & Dekker, 2013). These DNA domains are organized into transcriptionally active chromatin domains enriched for active epigenetic marks (e.g. H3K9Ac), or repressed chromatin domains enriched for repressive epigenetic marks (e.g. H3K27me3) at gene regulatory regions (Guelen et al., 2008; Lieberman-Aiden et al., 2009; Osborne et al., 2004). Transcription factors like GR form epigenetically marked chromatin loops that contain multiple genes that permit interactions among gene promoter and enhancer regions. These loops regulate transcription locally (John et al., 2011; Voss et al., 2011; Whirledge, Xu, & Cidlowski, 2013), But GR can also act globally via chromatin loops, targeting active genes to transcription factories and repressed genes to heterochromatin (Biddie, 2011; H. B. Li, Ohno, Gui, & Pirrotta, 2013). We have previously demonstrated histone epigenetic-post-translational marks to be present on immune-response genes affected by GC and also by psychological stress. GR was associated with these epigenetically marked genes and GC were shown to influence transcription by local control of gene accessibility (Eddy, Krukowski, Janusek, & Mathews, 2014; Krukowski et al., 2011; Mathews et al., 2011; Merkenschlager & Odom, 2013). Epigenetic marks of these types influence both chromatin organization and immune effector function (Kuznetsova et al., 2015; Olnes et al., 2016).

Aims and Hypotheses

It is well-established that psychological stress reduces NK cell immune function. This reduction is mediated by stress-induced release of GC, which can suppress immune function. Associated with suppression of a particular immune function are GC induced histone-epigenetic marks. Histone-epigenetic marks are responsible for the organization and compartmentalization of genomes into transcriptionally active euchromatin domains and that are localized to the interior of the nucleus. Transcriptionally silent heterochromatic regions are enriched with methylated epigenetic marks and are localized to the nuclear periphery. The **Purpose** of this investigation was to assess the influence of GC on H3K27me3 Chromatin Organization by measurement of that epigenetic mark. As well, the relationship of H3K27me3 Chromatin Organization to NK cell effector function, i.e. IFN gamma production, was determined. The **Central Hypothesis** is: H3K27me3 Chromatin Organization (CO) directly relates to NK cell immune function. In this investigation, CO will be assessed by measurement of the density and nuclear localization of histone post-translational epigenetic mark H3K27me3. Immune function will be assessed by measurement of NKCA as well as by the production of the immune effector molecule, IFN gamma. For Aim 1, the effects of stress hormone treatment on human peripheral blood mononuclear cells (PBMC) immune function will be assessed. Aim 2 will assess the effect of Dex on H3K27me3 CO. Aim 3 will assess relationships among H3K27me3 CO and the production of IFN gamma as a prime indicator of NK cell immune function. Should a relationship exist between H3K27me3 CO and NK cell immune function, then it is possible that CO may serve as an effective means for identification of GC induced immune dysregulation in NK cells.

Significance

It is the significant purpose of this project to evaluate H3K27me3 CO as an index associated with GC induced immune dysregulation, in that, GC related alteration of H3K27me3 CO may directly relate to the capacity of NK cells to carry out necessary immune function (IFN gamma production). Detection of GC induced alteration of H3K27me3 CO may provide a means by which to identify individuals with GC induced NK cell dysregulation. In this proposal we will couple an understanding of the effects of GC on the immune system with efficient and innovative high through-put technology, the Amnis ImageStream. It is a multispectral imaging flow cytometer, combining microscopic imaging with flow cytometry. It combines the per-cell information content provided by standard microscopy with the statistical significance afforded by large sample sizes common to standard flow cytometry. With this system, fluorescence intensity measurements are acquired as with a conventional flow cytometer; however, the system's imaging advantage is to locate and quantify the distribution of signals within a cell. This proposal could only be accomplished with this instrument and associated software and is an innovative aspect of this proposal.

CHAPTER TWO
METHODS AND MATERIALS

Cell Lines and Media

The human erythroleukemic-like cell line, K562, was obtained from the American Type Culture Collection, Rockville, MD. K562 cells were maintained in suspension in RPMI 1640 (Gibco Laboratories, Grand Island, NY) supplemented with 10% FBS (Gibco Laboratories, Grand Island, NY), 100 units/ml penicillin, 100ug/ml streptomycin (Whittaker M. A. Bioproducts, Walkersville, MD), 0.1 Mm non-essential amino acids and 2 Mm L-glutamine (Gibco Laboratories, Grand Island, NY). For *in vitro* human peripheral blood mononuclear cell (PBMC) experiments, cells were maintained in complete RPMI media identical to that used for K562 cells.

Subject Recruitment

Healthy volunteers participated in this study and were excluded if they had an immune-based disease, were substance abusers, had a history of acute infection, or were taking corticosteroids. This study was approved by the Loyola University Medical Center Institutional Review Board for the Study of Human Subjects. All procedures were carried out with the understanding and written consent of the participants.

***In vitro* Cellular Treatment of Human PBMC**

Whole blood was collected in sterile heparinized tubes and processed immediately. Heparinized peripheral blood was overlaid onto Ficoll/Hypaque and

centrifuged at 400 x g for 25 min. PBMC at the interface were extracted and washed twice in phosphate buffered saline (PBS) (Gibco, Grand Island, NY) prior to any treatment or phenotypic analysis. PBMC were then cultured at a concentration of 1×10^6 cells/ml in RPMI in the presence or absence of 10^{-6} M dexamethasone (Dex) (Sigma Aldrich, St. Louis, MO) or 10^{-6} M norepinephrine (NE) (Sigma Aldrich, St. Louis, MO) for 24 hr in 24 well plates. After treatment, cells were pooled, washed with RPMI and 1×10^6 cells were used for each analysis. Cell number and viability were determined by exclusion of 0.1% Trypan blue after isolation and after treatment. Viability was maintained between 90 and 95% in all experiments.

Natural Killer Cell Activity (NKCA)

K562 tumor cells were radioactively labeled with 100 uCi of [^{51}Cr] (New England Nuclear, Boston, MA). Radiolabeled K562 cells were washed and then incubated for 4 hr with PBMC. Following incubation, the supernatants were removed using a Skatron harvesting press (Skatron Inc., Sterling, VA) and the associated radioactivity was determined. Effector to target ratios for NKCA were 50, 30, 20, 10, and 5:1.

Results were expressed as % cytotoxicity and calculated by the formula:

$$\% \text{ Cytotoxicity} = \frac{(\text{experimental DPM}^*) - (\text{minimum DPM})}{(\text{maximum DPM}) - (\text{minimum DPM})} \times 100.$$

All experimental means were calculated from triplicate values.

*DPM=disintegrations per minute.

Measurement of IFN gamma by ELISA

1x10⁶ human PBMC were treated with Dex, NE, or left untreated. At the time of treatment, cells were activated with PMA/PHA (PMA @ 20ng/well; PHA @ 0.05%/well) and incubated for 48 hr at 37°C. Cell supernatants were then collected for analysis via ELISA (R&D Systems, Minneapolis, MN) according to the manufacturer's instructions.

Intracellular Staining of Human PBMC

After 24 hr, 1x10⁶ Dex treated or untreated PBMC were aliquoted into fluorescent activated cell sorting (FACS) tubes. The cells were washed twice with phosphate buffered saline (PBS) (Gibco, Grand Island, NY), then activated with lymphocyte activation cocktail (LAC) (BD Pharmingen, San Jose, CA) for 4 hr at 37°C. LAC contains PMA, ionomycin and brefeldin A. After activation, surface antibodies were added for 30 min on ice and agitated every 15 min to identify PBMC sub-populations. Surface stain antibodies included anti-CD3 (APCCy7 conjugated) (BD Biosciences San Jose, CA) and anti-CD56 (BV421 conjugated), (BD Biosciences, San Jose, CA). PBMC were then washed twice in 0.1% bovine serum albumin (BSA) (Sigma Aldrich, St. Louis, MO) in PBS. PBMC were then fixed and permeabilized with Cytotfix/Cytoperm solution (BD Pharmingen, San Jose, CA) for 20 min at 4°C. Then washed twice with Perm/Wash Buffer (BD Pharmingen, San Jose, CA). PBMC were then stained with antibodies specific for intracellular molecules of interest for 1 hr at 4°C. Intracellular antibodies included anti- IFN gamma (PE conjugated) (BD Biosciences, San Jose, CA) and anti-H3K27me3 (APC conjugated) (Cell Signaling, Beverly, MA). PBMC were then washed twice with Perm/Wash buffer. After wash the FACS tubes were then briefly vortexed and PBMC were transferred into 1.5 ml Eppendorf tubes. The tubes were then centrifuged, excess liquid was removed by pipet, and cells were resuspended in 50µl of 0.1% BSA in PBS to be analyzed with

the Amnis ImageStream (EMD Millipore, Billerica, MA) equipped with Inspire software. 10,000 events were collected and analyzed with ImageStream IDEAS software (EMD Millipore, Billerica, MA).

IDEAS Software Analysis of H3K27me3 in PBMC

The Inspire software simultaneously collects six images from each cell that passes through the instrument. These images include 5 fluorescence images and one bright field image stored as raw image files (.rif). Single fluorochrome files were collected and then used to generate compensation matrices and compensated image files (.cif). From the compensated image files, data analysis files (.daf) were created and analyzed for H3K27me3 localization. All acquired cells were plotted as histograms of the gradient root mean square of the bright field image, which measured the sharpness of the bright field image. Focused cells were then analyzed by a scatter plot of the aspect ratio (roundness of the cells) and area (size of the cells) to insure only individual lymphocyte analysis. CD56⁺ CD3⁻ cells were identified as NK cells. NK cells from both the Dex treated and untreated cell populations were visually analyzed for H3K27me3 localization.

Automation of H3K27me3 Localization with IDEAS Software

An automated technique was developed within the IDEAS software that allowed for analysis of H3K27me3 localization in every NK cell that passed through the flow cell. The automated technique provided a high throughput analysis of H3K27me3 localization within the nuclei of NK cells. The automated technique was created by merging the compensated image files (.cif) of the untreated and Dex treated NK cells into one data analysis file (.daf). Data analysis was performed with the Feature Finder program within the IDEAS software package. The Feature Finder program provided multiple image-based parameters that included: size,

location, shape, and texture (local intensity variations in the image) that enabled discrimination between cells based on their appearance. Additionally, the Feature Finder program calculated a statistic (termed Rd) that quantified the degree of discrimination of Peripheral H3K27me3 localization and Non-peripheral H3K27me3 localization in the NK cell population. Briefly, the merged data analysis file was initially analyzed to identify cells in focus. All NK cells were H3K27me3⁺. Then, two truth populations of cells were identified based on morphology. In this investigation, the truth populations were NK cells that had Peripheral H3K27me3 localization and NK cells that did not have Peripheral H3K27me3 localization (Non-peripheral H3K27me3 localization). 25 representative cells were tagged for each truth population. The truth populations in this study were based on localization of H3K27me3 regardless of H3K27me3 intensity to insure that feature selection was based on the localization of H3K27me3 within NK cell nuclei.

Confirmation that H3K27me3 Modulation and H3K27me3 Bright Detail Intensity (BDI) Differentiate Peripheral and Non-peripheral H3K27me3 Localization in NK Cell Nuclei

The Feature Finder identified H3K27me3 Modulation as well as H3K27me3 Bright Detail Intensity (BDI) as two features that discriminated Peripheral and Non-peripheral localization of H3K27me3. Modulation measured the intensity range of an image, normalized between 0 and 1. A numerically large Modulation value close to 1 identified a nucleus with areas of bright fluorescence intensity and also areas of weak to no intensity of H3K27me3. Modulation of H3K27me3 served as a quantitative value that represented the contour of H3K27me3 staining in individual nuclei. Modulation was calculated as: $\text{Modulation} = \frac{\text{Max Pixel} - \text{Min Pixel}}{\text{Max Pixel} + \text{Min Pixel}}$. Bright Detail Intensity quantified the local fluorescence density at a radius of 3 pixels (BDI). The BDI feature scanned the nucleus for bright spots, areas of increased density of H3K27me3 staining, within a 3 pixel radius, then eliminated any background staining and

reported the mean intensity of the bright spots within the nucleus. A numerically large BDI identified H3K27me3 with high density over a 3 pixel radius. These two features provided detailed information regarding H3K27me3 localization and density within NK cell nuclei.

H3K27me3 Modulation and H3K27me3 BDI were plotted for Dex treated and untreated NK cells. H3K27me3 Modulation Intervals (groups of individual NK cells with similar Modulation of H3K27me3) were analyzed in 10% increments of the maximum H3K27me3 Modulation present within the NK cell population. Confirmation that H3K27me3 Modulation and H3K27me3 BDI discriminated between Peripheral H3K27me3 localization and Non-peripheral H3K27me3 was accomplished by in-depth visual inspection (>2000 NK cells analyzed) of H3K27me3 localization from untreated and Dex treated NK cells in each H3K27me3 Modulation Interval derived from six independent samples. Representative images of H3K27me3 localization from each H3K27me3 Modulation Interval (taken at the Modulation midpoint of each interval) were visually assessed within H3K27me3 Modulation Intervals. Fifty cells from each H3K27me3 Modulation Interval in both untreated and Dex treated NK cells from six independent samples were assessed. If less than 50 NK cells were detected in the H3K27me3 Modulation Interval, all were counted. The percentage of NK cells within each Modulation Interval that had H3K27me3 localization similar to the representative image was recorded.

IDEAS Analysis of H3K27me3 Modulation Interval IFN gamma Production in NK Cells

H3K27me3 Modulation Interval IFN gamma production (measured as H3K27me3 Modulation Interval IFN gamma) in NK cells was calculated by the following equation:
 H3K27me3 Modulation Interval mean IFN gamma x % of NK cells for each H3K27me3 Modulation Interval. This resulted in H3K27me3 Modulation Interval IFN gamma values that

represented the level of IFN gamma within of the NK cells within each H3K27me3 Modulation Interval and served as an index of immune function for those NK cells.

Calculation of H3K27me3 Modulation Interval Chromatin Organization (CO)

H3K27me3 Modulation Interval CO was calculated with the following equation: mean H3K27me3 Modulation x mean H3K27me3 BDI x % of NK cells for each H3K27me3 Modulation Interval. Given that the H3K27me3 Modulation is normalized between 0 and 1, while the H3K27me3 BDI score can range from 1- 100,000, other mathematical manipulation of the scores would have resulted in H3K27me3 BDI dominating the analysis. Multiplication of the values equalized the weight given to both H3K27me3 Modulation and H3K27me3 BDI. Multiplication of H3K27me3 Modulation and H3K27me3 BDI with the percentage of NK cells within each H3K27me3 Modulation Interval resulted in a H3K27me3 Modulation Interval CO value that was representative of the amount of NK cells detected in each H3K27me3 Modulation Interval. H3K27me3 Modulation Interval CO was compared between Dex treated and untreated NK cells for each H3K27me3 Modulation Interval and served as an index to the effects of Dex on H3K27me3 CO throughout the entire NK cell population.

Calculation of H3K27me3 Global CO and Global IFN gamma Production

For each H3K27me3 Modulation Interval an H3K27me3 Modulation Interval CO value was calculated as: $\text{H3K27me3 Modulation Interval CO} = \text{mean H3K27me3 Modulation} \times \text{mean H3K27me3 BDI value} \times \% \text{ NK cells in the H3K27me3 Modulation Interval}$. Global H3K27me3 CO for the entire cell population was calculated as a summation of the 10 H3K27me3 Modulation Interval CO values.

H3K27me3 Modulation Interval IFN gamma was calculated as: $\text{H3K27me3 Modulation Interval IFN gamma MFI} = \text{mean IFN gamma MFI} \times \% \text{ NK cells in the H3K27me3 Modulation Interval}$

Interval. Global IFN gamma MFI for the entire population was calculated as the summation of the 10 H3K27me3 Modulation Interval IFN gamma values.

Single value Global H3K27me3 CO and single value Global IFN gamma MFI provided quantified values that permitted the direct assessment of the effects of Dex treatment on Chromatin Organization and IFN gamma production in NK cells. Such values provide an assessment measure by which to compare separate populations of NK cells for the effects of Dex on both H3K27me3 Chromatin Organization and immune function.

Statistical Analyses

All statistical analyses were performed with the Statistical Package for the Social Sciences (SPSS) software. Statistical analysis of all H3K27me3 Modulation Interval comparisons were compared by Student's t-test. NKCA was analyzed by group repeated measure ANOVA with Tukey HSD *post hoc* tests to determine differences between Dex treated and untreated PBMC. IFN gamma production by ELISA was analyzed by ANOVA with Tukey HSD *post hoc* tests to determine significant differences between Dex treated, NE treated, and untreated PBMC. All other analyses were compared by either Student's t-test, or Paired student's t-test as designated. Relationships were analyzed by Pearson r in SPSS. For all statistical tests $p < 0.05$ was set for significance.

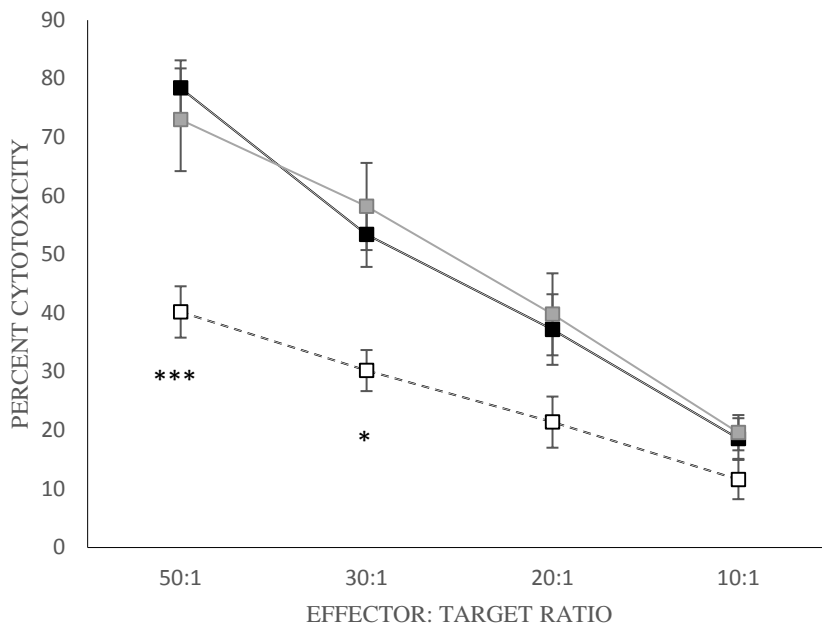
CHAPTER THREE

RESULTS

Effects of Dexamethasone (Dex) and Norepinephrine (NE) on PBMC Natural Killer Cell Activity (NKCA)

Both Dex and NE are reported to influence natural killer cell function. The two best characterized functional activities of human NK cells are NKCA and IFN gamma production. The effect of Dex and of NE on PBMC NKCA for tumor targets was assessed in Figure 1. PBMC were either untreated, or treated with Dex or NE (10^{-6} M) for 24 hr. (Varying Dex and NE concentrations (10^{-5} - 10^{-7} M) were evaluated, with maximum effect observed at 10^{-6} M for Dex with no effect for NE at 24 hr for any tested concentration. (Data are not shown.) A one-way group repeated measures ANOVA of the % Cytotoxicity of the effector to target ratios identified a significant effect of treatment on NKCA at the $p < 0.05$ level for the three conditions [$F(1, 2) = 6.971, p = 0.011$]. *Post hoc* Tukey HSD tests indicated significant differences in the means of Dex treated and untreated PBMC at the 50:1 and 30:1 effector to target ratios. NE had no demonstrable effect on the NKCA of PBMC. These data demonstrated that Dex but not NE reduced PBMC NKCA.

Figure 1. Effect of Dexamethasone (Dex) and Norepinephrine (NE) on NKCA of PBMC.



NKCA expressed as percent cytotoxicity for effector to target ratios of 50:1, 30:1, 20:1, and 10:1. Untreated PBMC are depicted in the black boxes, NE treated PBMC are depicted in the gray boxes, and Dex treated PBMC are depicted in the open boxes. Data represents the mean cytotoxicity of six individuals \pm SEM. Data were analyzed by one-way repeated measure ANOVA to determine differences among groups over all 4 effector to target ratios. *Post hoc* Tukey HSD analyses were then used to determine differences between Dex, NE, or untreated PBMC within each effector to target ratio. * = $p < 0.05$, *** = $p < 0.005$ comparison of Dex or NK treated and untreated PBMC.

Effects of Dex and NE on IFN gamma Production by PBMC and CD3⁺CD56⁺ NK Cells

The effect of Dex and of NE on NK cell IFN gamma production was assessed in two ways, ELISA measured PBMC production, or measurement of cytoplasmic mean fluorescence intensity levels (MFI) in NK cells. PBMC were either untreated or treated with Dex or NE (10^{-6} M) and activated for 48 hr. (As above, varying Dex and NE concentrations (10^{-5} - 10^{-7} M) were evaluated, with maximum effect observed at 10^{-6} M for Dex and no effect for NE at any tested concentration. Data are not shown.) There was a significant effect of treatment on IFN gamma production at the $p < 0.05$ level for the three conditions [$F(2, 18) = 5.039$, $p = 0.018$]. *Post hoc*

Tukey HSD tests indicated significant reduction in IFN gamma production in Dex treated PBMC when compared to untreated PBMC. While no effect was observed for NE. See Table 1. Further, Dex treated CD3⁻ CD56⁺ NK cells (NK) had significantly reduced cytoplasmic IFN gamma mean MFI when compared to untreated cells. Taken together, these data and those in Figure 1 demonstrate Dex to decrease PBMC NKCA and IFN gamma production. NE had no such effect. The effect of Dex on PBMC was likely due to NK cells in that NKCA in short term assay is mediated by such lymphocytes. IFN gamma can be produced by multiple lymphocyte populations, but reductions in IFN gamma MFI for lymphocytes demonstrates the effect on NK cells. Since no apparent effect on NK cell function was observed for NE, no further analysis was considered.

Table 1. Effect of Dex and NE treatment on IFN gamma production by PBMC and by NK cells

	Untreated	NE ⁻⁶ M	Dex ⁻⁶ M
IFN gamma (ng/ml)	4.631 +/- 1.368	3.198+/- 1.797	0.128 +/- .087*
IFN gamma (MFI)	3,498+/-1236	ND	2,303+/-814*

PBMC IFN gamma production, as ng/ml was measured by ELISA. Data represent the mean IFN gamma production by PBMC from six individuals +/- SEM. Data were analyzed by one-way ANOVA with Tukey HSD *post hoc* analysis, * = p < 0.05, comparison of Dex treated and untreated PBMC. No difference observed between untreated and NE treated PBMC. NK cell (CD3⁻CD56⁺) IFN gamma production was measured by mean fluorescence intensity (MFI) by Amnis ImageStream. Data represents the mean IFN gamma MFI from six individuals +/- SEM. Data were analyzed by Paired Student's t-test. * = p < 0.05 Dex treated NK cells compared to untreated NK cells. ND = not determined.

Effect of Dex on H3K27me3 Levels in NK Cells

Previous NK cell investigations have demonstrated Dex to modify histone post-translational epigenetic marks. Those modified epigenetic marks were shown to be directly associated with NK cell functions including NKCA and IFN gamma production [55-57]. One well characterized epigenetic mark is H3K27me3, which is associated with repressed gene expression and with the heterochromatic regions of the nucleus [61, 62]. Therefore, PBMC were either treated or not with Dex for 24 hr and H3K27me3 MFI was assessed in the NK cells. Dex treatment significantly increased the intensity of NK cell H3K27me3 immunofluorescence (as judged by MFI) when compared to untreated cells ($p < 0.005$). See Table 2. Such analysis provided evidence that Dex increased the detectable levels of the epigenetic mark, but did not provide specific information regarding the location of the increased immunofluorescent intensity within individual cells. To analyze the cellular location of the epigenetic mark, high through-put technology was employed, the Amnis ImageStream. With this instrument, fluorescence intensity measurements can be acquired as with a conventional flow cytometer; however, the system's imaging advantage is to locate and quantify the distribution of fluorescence intensity within a cell.

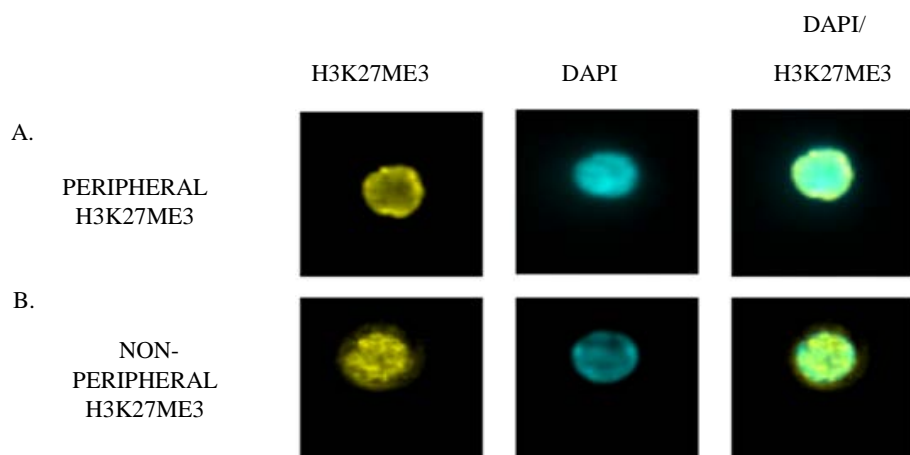
Table 2. Nuclear H3K27me3 mean fluorescence intensity (MFI) within dexamethasone (Dex) treated and untreated NK cells

	Untreated	Dex ⁻⁶ M	p
H3K27me3 Intensity	86,210+/- 30,480	100,000+/- 46,111	$p < 0.005$

Data represent the mean H3K27me3 MFI of NK cells from six individuals +/- SEM. Data were analyzed by Student's t-test.

Localization of H3K27me3 within Dex Treated NK Cells

When analyzed by the Amnis ImageStream, a population of lymphocytes within the Dex treated NK cells exhibited a distinct epigenetic pattern or phenotype. The cellular phenotype was H3K27me3 intense localization to the nuclear periphery, depicted in Figure 2A and termed Peripheral H3K27me3 localization. A cell that did not exhibit the phenotype is in Figure 2B in which H3K27me3 immunofluorescence appears to be diffusely distributed throughout the nucleus and termed Non-peripheral H3K27me3 localization. DAPI staining of the cells confirmed localization of the epigenetic mark to the nucleus. NK cells that exhibited Peripheral H3K27me3 localization were significantly more abundant in Dex treated NK cell populations than in untreated NK cell populations. See Table 3.

Figure 2. Nuclear localization of H3K27me3 in Dex treated and untreated NK cells.

Representative images of Peripheral and Non-peripheral H3K27me3 localization in NK cells. A. Peripheral localization of H3K27me3, the left panel depicts the immunofluorescent H3K27me3 localization in NK cell nuclei. Note the localization of H3K27me3 at the nuclear periphery, detected by yellow immunofluorescence. The center panel depicts the DAPI nuclear counterstain of the same NK cell depicted in the left panel. The right panel depicts the merged image illustrating H3K27me3 detection within the nucleus of NK cells. B. Non-peripheral H3K27me3 localization, the left panel depicts the immunofluorescent H3K27me3 localization in NK cell nuclei. Note H3K27me3 is not localized at the nuclear periphery, detected by yellow immunofluorescence. The center panel depicts the DAPI nuclear counterstain of the same NK cell depicted in the left panel. The right panel depicts the merged image illustrating H3K27me3 detection within the nucleus of NK cells.

Table 3. Localization of H3K27me3 within Dex treated and untreated NK cells.

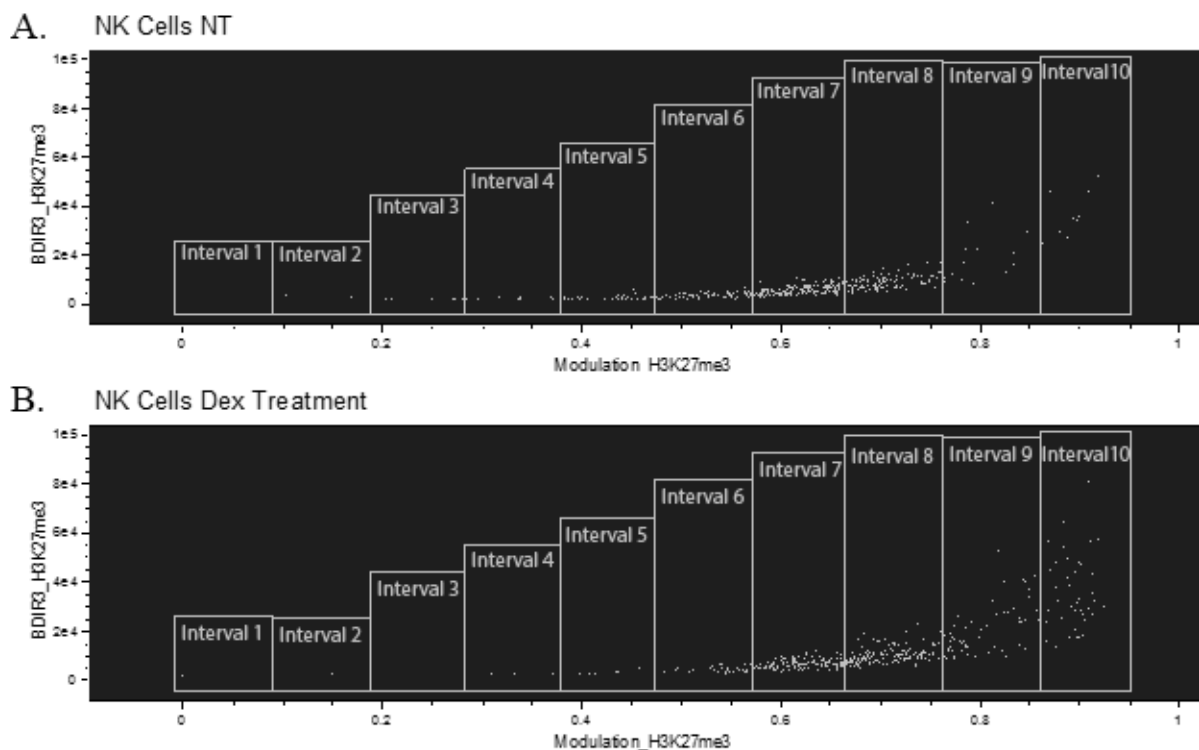
Phenotype	% Dex Treated	% Untreated	p
Non- Peripheral H3K27me3	40 +/- 2	64 +/- 2	<0.005
Peripheral H3K27me3	60 +/-2	36 +/- 2	<0.005

Visual inspection of 100 randomly selected NK cells for Peripheral and Non- Peripheral H3K27me3 localization in Dex treated and untreated cells. Data represent mean values of NK cells from six individuals +/- SEM. Data were analyzed by Student's t-test.

Localization and Density Quantification of NK Cell Nuclear H3K27me3

H3K27me3 localization and density was automated and quantified within a given cellular population by use of the Amnis ImageStream, Feature Finder program within the IDEAS software. The Feature Finder program does so by quantification of H3K27me3 Modulation as well as H3K27me3 Bright Detail Intensity (BDI). A numerically large Modulation value identifies a nucleus with areas of bright fluorescence intensity and areas of weak intensity. Values are normalized to a number between 0 and 1. Modulation serves as a quantitative value representing the contour of H3K27me3 staining within individual nuclei. Bright Detail Intensity quantifies the local fluorescence density at a radius of 3 pixels (BDI). A numerically large BDI value identifies a nucleus wherein the fluorescent signal is highly condensed locally. The relationship of these two Features, H3K27me3 Modulation and H3K27me3 BDI was assessed for an individual NK cell population (derived from a single individual) and those cells either Dex treated or not for 24 hr. See Figure 3. Each individual NK cell is represented by a single plotted point, with the population as a whole separated into H3K27me3 Modulation Intervals that represent 10% increments of the maximum H3K27me3 Modulation value of the NK cell population.

Figure 3. Relationship of H3K27me3 Modulation to H3K27me3 Bright Detail Intensity (BDI) within NK cells.

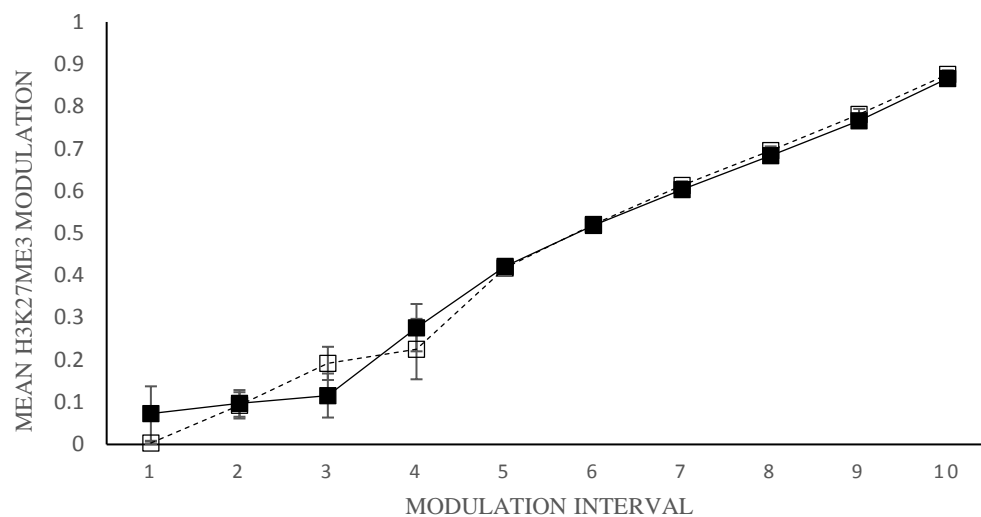


Relationship between H3K27me3 Modulation to H3K27me3 BDI in untreated NK cells. B. Relationship between H3K27me3 Modulation and H3K27me3 BDI in Dex treated NK cells. Definitions of H3K27me3 Modulation and H3K27me3 BDI are detailed in the Methods and Materials Section. H3K27me3 Modulation is plotted on the x-axis. While H3K27me3 BDI is plotted on the y-axis. Each dot represents an individual NK cell. H3K27me3 Modulation Intervals represent 10% increments of the maximum H3K27me3 Modulation value for an individual NK cell population derived from a single individual. NT = untreated.

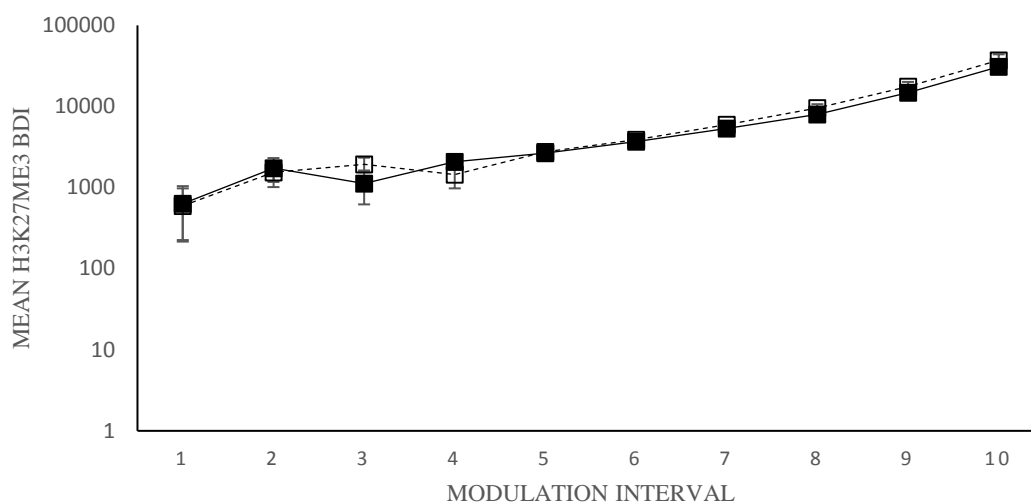
Mean H3K27me3 Modulation and mean H3K27me3 BDI were determined for each H3K27me3 Modulation Interval. When NK cell populations were derived from six separate individuals and Dex treated or not, H3K27me3 Modulation and H3K27me3 BDI of for each H3K27me3 Modulation Interval did not differ statistically between the untreated and Dex treated NK cells. See Figure 4.

Figure 4. H3K27me3 Modulation and H3K27me3 BDI of Dex treated and untreated NK cells for each H3K27me3 Modulation Interval.

A.



B.



The mean H3K27me3 Modulation of NK cells within each H3K27me3 Modulation Interval. Data represents the mean of six individuals +/-SEM. Dex treated NK cells are depicted in the open squares and untreated NK cells are depicted in the closed squares. B. The mean H3K27me3 BDI of NK cells within each H3K27me3 Modulation Interval. Data represents the mean of six individuals +/- SEM. Dex treated NK cells are depicted in the open squares while untreated NK cells are depicted in the closed squares. Data were analyzed by Student's t-test for each H3K27me3 Modulation Interval. None were significant.

Data from Figure 3 and Figure 4 do indicate that as H3K27me3 Modulation increased there was a concomitant increase in H3K27me3 BDI. A significant positive relationship between H3K27me3 Modulation and H3K27me3 BDI in both Dex treated NK cells ($r = 0.669$, $p < 0.005$) and untreated NK cells ($r = 0.666$, $p < 0.005$) was observed. This relationship was observed in NK cells from a single individual, but is representative of relationships seen in NK cells from six individuals. See Table 4. These data demonstrated that with increased H3K27me3 Modulation there was a concomitant increase in H3K27me3 BDI.




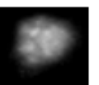
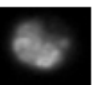



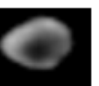
Table 4. Relationship between H3K27me3 Modulation and H3K27me3 BDI in untreated and Dex treated NK cell populations from six individuals.

	Untreated NK cells r=	p=	Dex NK cells r=	p=
Sample 1	0.652	0.0005	0.714	0.0005
Sample 2	0.587	0.0005	0.648	0.0005
Sample 3	0.666	0.0005	0.669	0.0005
Sample 4	0.611	0.0005	0.655	0.0005
Sample 5	0.690	0.0005	0.693	0.0005
Sample 6	0.671	0.005	0.799	0.0005

*Note $p < 0.05$ was considered significant.

In Table 5 representative images for each H3K27me3 Modulation Interval are depicted. (The representative images were taken from the H3K27me3 Modulation midpoint of each Modulation Interval.) It is apparent that for Modulation Intervals 8-10 a majority of NK cells had Peripheral H3K27me3 localization in both Dex treated and untreated NK cells from six independent samples. These data indicated that with increased H3K27me3 Modulation and H3K27me3 BDI there is an increase in Peripheral nuclear localization of H3K27me3 for both Dex treated and untreated NK cells. The percentage of NK cells with similar H3K27me3 nuclear localization within the H3K27me3 Modulation Intervals did not differ between Dex treated and untreated cells from six individual samples ($p > 0.05$).

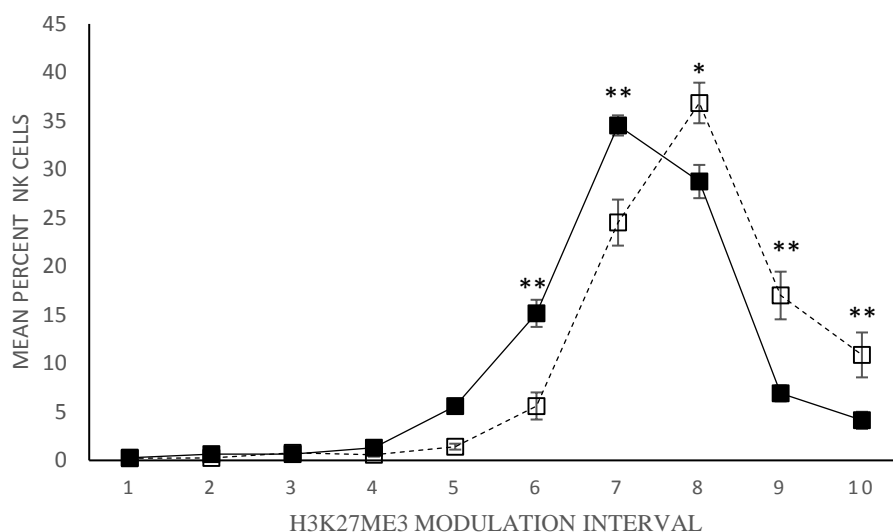
Table 5. Percentage of Dex and untreated NK cells within H3K27me3 Modulation Intervals with representative localization of H3K27me3.

	Interval2	Interval3	Interval4	Interval5	Interval6	Interval7	Interval8	Interval9	Interval10
									
Untreated NK	100+/- 0	100+/- 0	100+/- 0	100+/- 0	100+/- 0	95+/- 5	75+/- 8	89+/- 4	90+/- 5
Dex ^{-6M} NK	100+/- 0	100+/- 0	100+/- 0	100+/- 0	100+/- 0	80+/- 9	86+/- 8	95+/- 3	100+/- 0

Representative images of H3K27me3 localization in NK cell nuclei. Visual inspection of 50 cells/ H3K27me3 Modulation Interval to determine Peripheral or Non-peripheral H3K27me3 localization within each H3K27me3 Modulation Interval. Analysis was not performed in H3K27me3 Modulation Interval 1 due to the absence of cells. Data represents the mean percentage of cells with H3K27me3 localization similar to the representative image of the H3K27me3 Modulation Interval for the NK cells of six individuals +/- SEM.

However, calculation of the percentage of NK cells in each H3K27me3 Modulation Interval demonstrated a significant increase in H3K27me3 Modulation Intervals 8, 9, and 10 for NK cells treated with Dex when compared to untreated cells. There was also a significant reduction in the percentage of NK cells in H3K27me3 Modulation Intervals 6 and 7 for NK cells treated with Dex when compared to untreated cells. See Figure 5. Taken together these data demonstrate Dex to increase the percentage of cells in H3K27me3 Modulation Intervals 8-10, and decrease the percentage of cells in H3K27me3 Modulation Intervals 6 and 7. Further, increased H3K27me3 Modulation and increased H3K27me3 BDI directly related to nuclear Peripheral localization of H3K27me3.

Figure 5. NK cell percentage within each H3K27me3 Modulation Interval.



Percentage of NK cells present in each H3K27me3 Modulation Interval was determined for NK cells derived from six individuals. Untreated NK cells are depicted by the closed boxes. Dex treated NK cells are depicted by the open boxes. Data are means of six individuals \pm SEM. The data were analyzed by Student's t-test for each H3K27me3 Modulation Interval. * $p < 0.05$, ** $p < 0.01$.

Relationships of H3K27me3 Modulation and H3K27me3 BDI to Cytoplasmic IFN gamma Levels in NK Cells

In Dex treated NK cells there was a significant relationship between H3K27me3 Modulation and cytoplasmic IFN gamma MFI ($r = -0.344$, $p < 0.005$). No significant relationship was observed for H3K27me3 Modulation and cytoplasmic IFN gamma in untreated NK cells ($r = -0.030$, $p = 0.783$). These relationships were for the individual's NK cell population presented in Figure 3, and representative of relationships observed in six separate individuals. See Table 6. These data demonstrate a negative relationship between H3K27me3 Modulation and IFN gamma levels in Dex treated NK cells. There was also a significant relationship between H3K27me3 BDI and cytoplasmic IFN gamma within the Dex treated NK cell population ($r = -0.236$, $p < 0.005$). No significant relationship was observed within the untreated NK cell population ($r = -0.190$, $p = 0.09$). These relationships were representative of six separate individuals. See Table

7. These data demonstrate that increased H3K27me3 Modulation and increased H3K27me3 BDI relate to decreased IFN gamma production in Dex treated NK cells.

Table 6. Relationships between H3K27me3 Modulation and IFN gamma MFI in untreated and Dex treated NK cell populations from six individuals.

	Untreated NK cells r=	p=	Dex NK cells r=	p=
Sample 1	-0.213	0.10	-0.340	0.0005
Sample 2	-0.024	0.819	-0.159	0.05
Sample 3	0.030	0.783	-0.344	0.0005
Sample 4	-0.103	0.112	-0.243	0.0005
Sample 5	0.093	0.433	-0.556	0.0005
Sample 6	0.052	0.520	-0.671	0.0005

*Note p<0.05 was considered significant.

Table 7. Relationship between H3K27me3 BDI and IFN gamma MFI in untreated and Dex treated NK cell populations from six individuals.

	Untreated NK cells r=	p=	Dex NK cells r=	p=
Sample 1	-0.197	0.16	-0.241	0.0005
Sample 2	-0.161	0.118	-0.148	0.05
Sample 3	-0.190	0.09	-0.236	0.0005
Sample 4	-0.179	0.163	-0.167	0.005
Sample 5	0.084	0.362	-0.567	0.0005
Sample 6	0.022	0.787	-0.684	0.0005

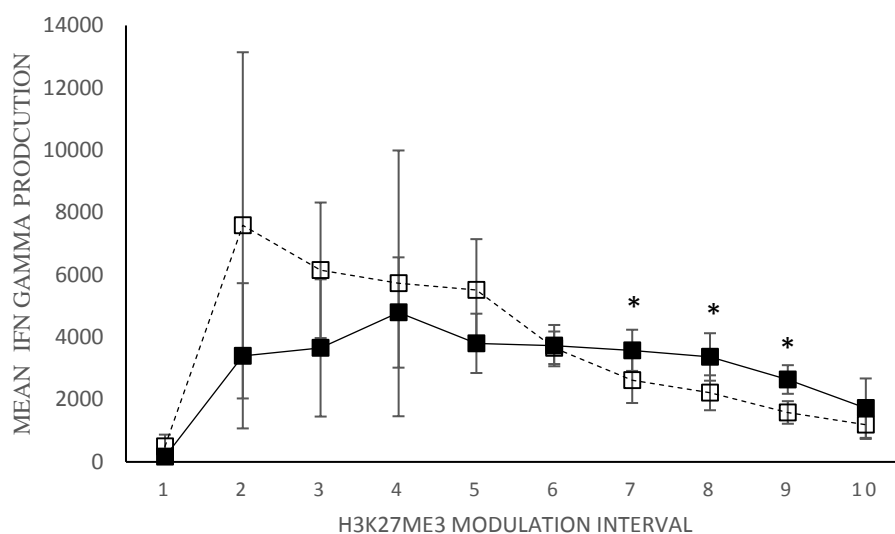
*Note p<0.05 was considered significant.

Quantification of H3K27me3 Modulation Interval IFN gamma Production in NK Cells

IFN gamma production values were calculated for each H3K27me3 Modulation Interval as: mean IFN gamma MFI x % NK cells detected in each H3K27me3 Modulation Interval. This resulted in H3K27me3 Modulation Interval IFN gamma values that were representative of the NK cells detected within each H3K27me3 Modulation Interval. H3K27me3 Modulation Interval IFN gamma values were then compared in Dex treated and untreated H3K27me3 Modulation Intervals. See Figure 6. Dex treatment significantly decreased the H3K27me3 Modulation

Interval IFN gamma in intervals 7, 8, and 9 when compared to untreated NK cells. There were no significant differences detected in H3K27me3 Modulation Intervals 1-6, or 10.

Figure 6. NK cell H3K27me3 Modulation Interval IFN gamma Production



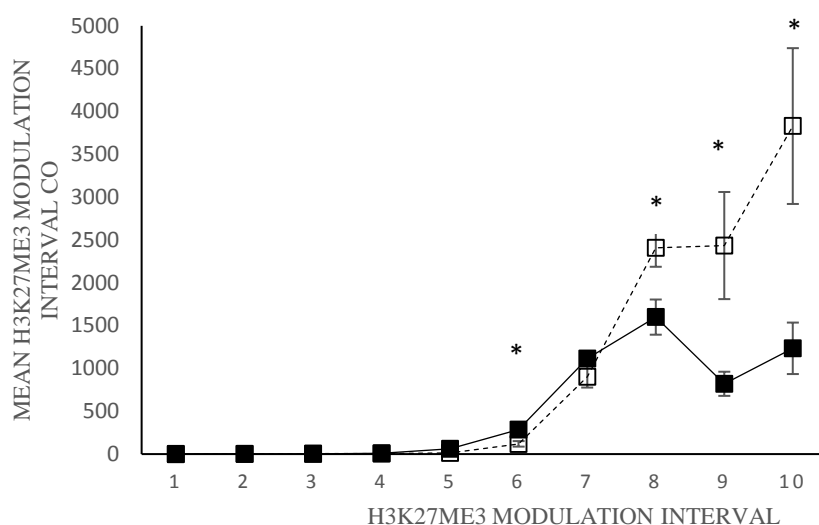
H3K27me3 Modulation Interval IFN gamma production for untreated NK cells is depicted in the closed boxes and for Dex treated NK cells, open boxes. H3K27me3 Modulation Interval IFN gamma was calculated as follows: H3K27me3 Modulation Interval mean IFN gamma MFI x % NK cells for each H3K27me3 Modulation Interval. Data are the mean of six individuals +/- SEM. The data were analyzed by Student's t-test for each H3K27me3 Modulation Interval. *p < 0.05.

H3K27me3 Modulation Interval Chromatin Organization (CO) of Dex Treated and Untreated NK Cells

H3K27me3 Modulation and H3K27me3 BDI provide rapid, and high throughput quantification of the localization and density of H3K27me3 within the nucleus of individual NK cells. When combined with the percentage of NK cells within a particular H3K27me3 Modulation Interval, the mean H3K27me3 Modulation Interval Chromatin Organization (CO) value of the NK cells within each H3K27me3 Modulation Interval was calculated: mean H3K27me3 Modulation x mean H3K27me3 BDI x % NK cells in each H3K27me3 Modulation

Interval. A comparison of H3K27me3 Modulation Interval CO for Dex treated and untreated NK cells is shown in Figure 7. For H3K27me3 Modulation Intervals 8-10, (H3K27me3 Modulation Intervals with Peripheral H3K27me3 localization) Dex treated cells had a significant increase in H3K27me3 Modulation Interval CO when compared to untreated NK cells. These data demonstrate Dex to increase H3K27me3 CO and the increase is due to an increase in the percentage of NK cells that contained Peripheral H3K27me3 localization.

Figure 7. H3K27me3 Modulation Interval Chromatin Organization (CO) of Dex treated and untreated NK cells.

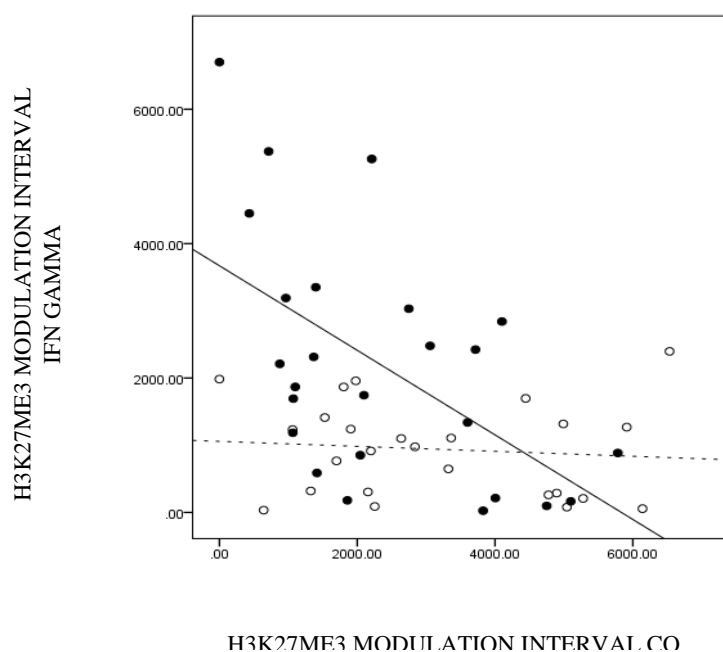


H3K27me3 Modulation Interval CO for untreated NK cells is depicted in the closed boxes and Dex treated NK cells, open boxes. H3K27me3 Modulation Interval CO for each H3K27me3 Modulation Interval was calculated as: mean H3K27me3 Modulation x mean H3K27me3 BDI x Percentage of NK cells within each H3K27me3 Modulation Interval. Data are the mean of six individuals +/- SEM. The data were analyzed by Student's t-test for each H3K27me3 Modulation Interval. * = $p < 0.05$.

For six separate NK cell populations (derived from 6 separate individuals), relationships among H3K27me3 Modulation Interval CO and H3K27me3 Modulation Interval cytoplasmic IFN gamma were evaluated. See Figure 8. A significant negative relationship ($r = -0.557$, $p = 0.004$) was found between Modulation Interval H3K27me3 CO and Modulation Interval IFN gamma MFI in Dex treated NK cells while no association was observed for untreated NK cells ($r = -$

0.097, $p = 0.638$). Data for H3K27me3 Modulation Intervals 6-10 were analyzed in that no difference in H3K27me3 Modulation Interval IFN gamma 1-5 was noted. Further, H3K27me3 Modulation Intervals 6-10 contained the majority of NK cells within each subject. In Dex treated NK cells, Modulation Intervals 6-10 contained 95% +/- 1.7% of the entire NK cell population. While in untreated NK cells, H3K27me3 Modulation Intervals 6-10 contained 89.5% +/- 1.7% of the entire NK cell population.

Figure 8. Relationship of H3K27me3 Modulation Interval Chromatin Organization (CO) to H3K27me3 Modulation Interval IFN gamma production in Dex treated and untreated NK cells.



Relationship of H3K27me3 Modulation Interval Chromatin Organization (CO) to H3K27me3 Modulation Interval IFN gamma production in Dex treated and untreated NK cells. Untreated NK cells are depicted in the open circles and Dex treated NK cells are depicted in the closed circles. The relationship between H3K27me3 Modulation Interval CO and H3K27me3 Modulation Interval IFN gamma production for untreated cells is depicted by the hashed line ($r = .097$, $p = 0.638$). The relationship between H3K27me3 Modulation Interval CO and H3K27me3 Modulation Interval IFN gamma production of Dex treated NK cells is depicted by the solid line ($r = -0.557$, $p = 0.004$). Data for H3K27me3 Modulation Intervals 6-10 for six individuals, comprise the Figure.

H3K27me3 Global Chromatin Organization (CO) of Dex Treated and Untreated NK Cells with regard to NK cell IFN gamma Production

In order to make a direct comparison of NK cell populations, a H3K27me3 Global Chromatin Organization value was derived and is the summation of the 10 H3K27me3 Modulation Interval CO values. In this manner, a single value was assigned to an entire NK cell population and that value was then evaluated in the context of NK cell function (e.g. IFN gamma levels for the entire CD56+ NK cell population). See Table 4A. Dex treated NK cells had a significantly larger H3K27me3 Global CO value, which coincided with a significantly reduced Global IFN gamma value for the entire population of cells. Likewise, when H3K27me3 Global CO and Global IFN gamma were compared for the summation of data from H3K27me3 Modulation Intervals 6-10. See Table 4B. The results from the summations of H3K27me3 Modulation Intervals 1-10 were recapitulated. These data demonstrated that H3K27me3 Chromatin Organization was coincident with decreased NK cell function.

Table 8. H3K27me3 Global Chromatin Organization (CO) Value and Cytoplasmic IFN gamma levels for individual populations of NK cells.

A.	Untreated	Dex ⁶ M	p=	B.	Untreated	Dex ⁶ M	p=
H3K27me3	5,071+/-	9,383	0.006	H3K27me3	5,055+/-	9,696+	0.005
Global CO	504	+/-		Global CO	636	/-1360	
(H3K27me3 Modulation Interval 1-10)		1121		(H3K27me3 Modulation Interval 6-10)			
Cytoplasmic	3,382+/-	2,240	0.007	Cytoplasmic	3,008+/-	2,046+	0.001
IFN gamma	571	+/-		IFN gamma	550	/-488	
(H3K27me3 Modulation Interval 1-10)		446		(H3K27me3 Modulation Interval 6-10)			

A. H3K27me3 Global CO value for the entire cell population was calculated as the summation of the 10 H3K27me3 Modulation Interval H3K27me3 CO values. As well a Global IFN gamma value for the entire cell population was calculated as the summation of the 10 H3K27me3 Modulation Interval IFN gamma values. B. H3K27me3 Global CO was calculated as the summation of H3K27me3 Modulation Intervals 6-10. Global IFN gamma value was calculated as the summation of H3K27me3 Modulation Interval IFN gamma values from H3K27me3 Modulation Intervals 6-10. NK cells were derived from 6 individuals +/- SEM. Dex and untreated NK cells were compared by Paired t-test.

CHAPTER FOUR

DISCUSSION

In this investigation dexamethasone (Dex) was shown to alter the H3K27me3 Global Chromatin Organization (CO) of NK cells. This alteration was evidenced by an increase in the intensity (as judged by mean fluorescent intensity, MFI) of the histone epigenetic, post-translational mark, H3K27me3. Increased H3K27me3 intensity was related to Peripheral H3K27me3 localization in individual NK cells. Peripheral localization was first determined by visual inspection and then by automated analysis of H3K27me3 Modulation and H3K27me3 BDI within individual NK cells. With increased H3K27me3 Modulation and increased H3K27me3 BDI there was intensified Peripheral H3K27me3 localization. With Dex treatment, the percentage of NK cells with Peripheral H3K27me3 localization was markedly increased, especially in H3K27me3 Modulation Intervals 8-10. This Peripheral H3K27me3 localization is consistent with heterochromatic DNA in which effected genes are repressed (Amendola & van Steensel, 2014; Grewal & Moazed, 2003).

Peripheral H3K27me3 localization was noted in untreated NK cells and this was not unexpected in that silenced genes are expected to have a heterochromatic localization (Andrulis, Neiman, Zappulla, & Sternglanz, 1998). Environmental factors including but not limited to diet (Sadhu et al., 2013), age (Bracken et al., 2007; Kawakami, Nakamura, Ishigami, Goto, & Takahashi, 2009), smoking (Sundar, Nevid, Friedman, & Rahman, 2014; Yang et al., 2008), previous psychological stressors (Eddy, Krukowski, Janusek, & Mathews, 2014; Krukowski et al., 2011), and alcoholic intake (Kim & Shukla, 2006) are known to effect epigenetic marks and

can contribute to the Peripheral H3K27me3 localization observed in untreated NK cell populations. However, it is clear is that Dex significantly increased the percentage of NK cells with increased Peripheral H3K27me3 localization and H3K27me3 BDI, suggesting that glucocorticoids drive the localization and density of H3K27me3 toward the nuclear periphery. Taken together, these data indicate that glucocorticoid treatment increases H3K27me3 intensity. The increase in the repressive epigenetic mark H3K27me3 increases the localization of H3K27me3-marked DNA toward the nuclear periphery in NK cells that is consistent with repressed, heterochromatic DNA. It was previously known that epigenetic marks compartmentalize chromatin into actively transcribed euchromatic and repressed heterochromatic domains (Martin & Zhang, 2005; Misteli, 2007), however to the authors' knowledge, this is the first time that GC induced global alterations of nuclear H3K27me3 localization has been visualized.

Increased Peripheral localization of H3K27me3 was directly related to reduced production of intracellular IFN gamma. A negative relationship was observed between H3K27me3 Modulation Interval CO and IFN gamma in H3K27me3 Modulation Intervals 6-10 in Dex treated NK cells that was not observed in untreated NK cells. H3K27me3 Modulation Intervals 6-10 were chosen to analyze the relationship between H3K27me3 Modulation Interval CO and IFN gamma because there were no observed differences in IFN gamma production for H3K27me3 Modulation Intervals 1-5 between Dex treated and untreated NK cells. Further, the majority of NK cells were detected in H3K27me3 Modulation Intervals 6-10. The calculation of H3K27me3 Global CO and Global IFN gamma values, in which Dex treated NK cells had significantly higher H3K27me3 Global CO and a concomitant decrease in NK cell IFN gamma production. These data indicate that Dex treatment alters H3K27me3 CO within NK cells by increasing the Peripheral localization

and density of H3K27me₃-marked chromatin and the alteration of H3K27me CO is directly related to reduced IFN gamma production. Hence, the Peripheral localization and density of H3K27me₃ (H3K27me₃ CO) within NK cells may be an indicator of GC induced NK cell dysregulation. The finding that H3K27me₃ CO is directly related to effector function is further substantiated by a recent study in hepatocellular carcinoma, in which increased H3K27me₃ localization to the nuclear periphery is correlated to an aggressive tumor subgroup of HCC (Hayashi, et al., 2014). The results described in this manuscript are the first to describe a correlation between glucocorticoid induced alteration of H3K27me₃ Global Chromatin Organization and reduced NK cell IFN gamma production.

This investigation was accomplished by coupling an evaluation of the effects of Dex on NK cells with an efficient and innovative high through-put technology, the Amnis ImageStream. It achieves high through-put capacity as a multispectral imaging flow cytometer, combining microscopic imaging with flow cytometry. It can image up to 100 cells/sec, with simultaneous acquisition of 6 images per cell, including bright field and fluorescent intensities. It combines the per-cell information content provided by standard microscopy with the statistical significance afforded by large sample sizes common to standard flow cytometry. Localization of H3K27me₃ signal intensity was measured with the Amnis ImageStream IDEAS software Modulation feature, which quantifies signal intensity distribution within the nucleus, normalized as a number between 0 and 1. H3K27me₃ Modulation served as a quantitative value representing the contour of H3K27me₃ staining in individual nuclei. Increased H3K27me₃ Modulation was correlated with increased Peripheral localization of H3K27me₃. H3K27me₃ BDI identified increased density of H3K27me₃ in individual nuclei. With increased H3K27me₃ BDI there was an increase in density of H3K27me₃ at the nuclear periphery. Hence, H3K27me₃ Modulation and

H3K27me3 BDI were utilized to develop a H3K27me3 Chromatin Organization value to ascertain the degree of Peripheral localization of H3K27me3 and density of H3K27me3 within NK cell nuclei that could then be easily compared to immune function (i.e. IFN gamma).

Chromatin organization both reflects and impacts transcriptional regulation and is responsive to physiological stimuli (Misteli, 2007; Schneider & Grosschedl, 2007). Chromatin organization at the nuclear periphery, affects gene transcription, as well as inter- and intra-chromosomal gene clustering (Misteli, 2007; Schneider & Grosschedl, 2007) and is an important site for both active and repressed gene transcription (Akhtar & Gasser, 2007; Egecioglu & Brickner, 2011).

Each chromosome within the nucleus occupies a defined nuclear territory with spatial domains dependent upon distinct structural and functional states. These are; euchromatin, which is loosely packed and contains transcriptionally active loci, and heterochromatin, which is highly compact and transcriptionally silent (Misteli, 2007). At the nuclear periphery euchromatin tends to localize to the nuclear pore complex (NPC) while heterochromatin tends to localize to the lamina (Belmont, Zhai, & Thilenius, 1993; Schermelleh et al., 2008). Actively transcribed genes are tethered to the NPC (Arib & Akhtar, 2011; Blobel, 1985; Krull et al., 2010), which facilitates mRNA export (Brickner et al., 2012; Schmid et al., 2006). In close proximity to the NPC and associated with the nuclear lamina is heterochromatin (Green, Jiang, Joyner, & Weis, 2012; Van de Vosse et al., 2013), in which gene transcription is repressed (Light, Brickner, Brand, & Brickner, 2010). Hence, the nuclear periphery is a platform in which the more abundant heterochromatin is interrupted by the euchromatin associated with the NPC (Casolari et al., 2004; Green et al., 2012; Ikegami & Lieb, 2013; Light et al., 2010; Pascual-Garcia & Capelson, 2014; Taddei et al., 2006; Van de Vosse et al., 2013).

DNA regions marked by H3K27me3 are nucleosome compacted and when associated with the nuclear periphery are heterochromatic. These regions contain inaccessible regulatory elements, reduced transcription factor binding and are readily detected as a highly ordered structure within the three dimensional architecture of the nucleus (Amendola & van Steensel, 2014; Grewal & Moazed, 2003). Regions of DNA containing H3K27me3 form large compartments of topologically associated domains (TADs) containing tracts of DNA silenced by the polycomb-repressive complexes (PRC) (Dixon et al., 2012; Rao et al., 2014). These TADs dictate transcription of the genes contained within the TAD. Tri-methylation of lysine 27 on the exposed N-terminal tail of histone H3 (H3K27me3) is catalyzed by the methyl transferase Enhancer of Zeste Homolog 2 (Ezh2), which is a subunit of PRC2 (Margueron & Reinberg, 2011). Histone tri-methylation of H3K27 at the targeted nucleosome enhances the activity of PRC2 and with increased PRC2 methyl transferase activity, H3K27me3 marks propagate along the chromosome (Margueron et al., 2009). PRC2 and H3K27me3 recruit protein complexes that compact chromatin and epigenetically silence genes within that region of DNA (Margueron & Reinberg, 2011; Simon & Kingston, 2009; Spivakov & Fisher, 2007). These protein complexes include histone deacetylase 1 (HDAC1) (Tie, Furuyama, Prasad-Sinha, Jane, & Harte, 2001; van der Vlag & Otte, 1999) that reduces DNA accessibility by histone deacetylation (Haberland, Montgomery, & Olson, 2009) and is known to interact with PRC2 through EZH2 (van der Vlag & Otte, 1999).

We have previously demonstrated GC: GR to associate with HDAC1 and to repress IFN gamma production by NK cells (Bush, Krukowski, Eddy, Janusek, & Mathews, 2012; Krukowski et al., 2011). Reduction of IFN gamma production by Dex is associated with reduced histone acetylation at the *IFNG* promoter and with a quantitative reduction in *IFNG* mRNA

production (Krukowski et al., 2011). In this investigation we extend those observations by analysis of Dex effect on the repressive epigenetic mark, H3K27me3. We found Dex to not only increase detectable H3K27me3 within nuclei but also to increase localization of the epigenetic mark to the heterochromatic nuclear periphery. Such localization correlated with reduced IFN gamma production. Upon stimulation, mature NK cells are poised to produce IFN gamma within minutes to hours after stimulation (Stetson et al., 2003). Hence, the euchromatic localization of *IFNG* is likely at the NPC, for rapid mRNA nuclear export and active transcription. With increased glucocorticoids (e.g. during stress), GC: GR recruitment of PRC2 with tri-methylation of H3K27 and deacetylation by HDAC1, likely condense the chromatin domain containing *IFNG*, associating it with the nuclear lamina. GR binds to >10,000 sites within the human genome and glucocorticoids regulate the expression of hundreds of genes interacting over tens of kilobases (Olnes et al., 2016; Vockley et al., 2016). These long range interactions regulate multiple genes within TADS (Kuznetsova et al., 2015). Hence, the Dex induced extensive detection of H3K27me3 at the nuclear periphery likely reflects the heterochromatic localization of chromatin domains containing these repressed genes as well as *IFNG* (Galon et al., 2002; Wang et al., 2016).

The focus of this investigation was measurement of immune cell function by cytoplasmic assessment of IFN gamma production by individual NK cells. As described previously, NK cells are large, granular lymphocytes that are poised for rapid effector function (Stetson et al., 2003). NK cells belong to the family of group 1 innate lymphocytes (ILC1), their frequency approximates 10% in peripheral blood, and are functionally characterized by their cytotoxicity and their ability to produce cytokines (Vivier, Tomasello, Baratin, Walzer, & Ugolini, 2008) that shape the innate and adaptive immune responses (Vivier et al., 2011). However, the best-

characterized cytokine produced by NK cells is IFN gamma (Cooper et al., 2001), which is quickly released within minutes to hours after NK cell stimulation (Stetson et al., 2003). NK cell produced IFN gamma has many effects on the immune response, including induction of MHC class II molecules on antigen-presenting cells, activation of myeloid cells and induction of T helper 1 (TH1) cells (Morvan & Lanier, 2016). Macrophage activation by NK cell-derived IFN gamma has been shown to be essential for resistance to primary tumorigenesis. As such, IFN gamma production by NK cells is central to the optimal function of the immune system. Measurement of its production in NK cells is particularly important because the response to stimulus is essentially immediate and does not require longer term activation as would be required with T lymphocytes.

The relationship of psychological stress and the HPA axis is well established (Gotlieb et al., 2015). It is known that Dex, at therapeutic concentrations, is anti-inflammatory and as an immunosuppressive agent is used for the treatment of numerous autoimmune and inflammatory diseases (Boumpas, Chrousos, Wilder, Cupps, & Balow, 1993). Endogenous glucocorticoids also play a physiologic role in feedback inhibition of immune/inflammatory responses (Karin, 1998; Wilckens & De Rijk, 1997). Further, exogenous Dex at physiological concentrations has repeatedly been shown to markedly suppress human and animal NK immune function (Cox, Holbrook, & Friedman, 1983; Gatti, Cavallo, Sartori, Marinone, & Angeli, 1986; Krukowski et al., 2011; Shakhar et al., 2007; Witek-Janusek et al., 2008; Witek-Janusek, Gabram, & Mathews, 2007). Further, GC are known to suppress production of the cytokine, interferon (IFN) gamma, via glucocorticoid receptor (GR) activation (Ding, Yang, & Xu, 1989; Vieira, Kaliński, Wierenga, Kapsenberg, & de Jong, 1998; Visser et al., 1998) as well as reducing NKCA (Eddy et al., 2014; Krukowski et al., 2011) through GR interaction with immune effector loci. We have

also demonstrated that the effects of GC on NKCA and IFN gamma in NK cells *in vitro* is partially mediated by an epigenetic mechanism (Eddy et al., 2014; Krukowski et al., 2011). Based on the data presented herein it appears that in addition to these effects, Peripheral localization of the repressive epigenetic mark H3K27me3 is also influenced by Dex and that such localization is related to suppression of cytokine production.

In contrast, the effect of norepinephrine (NE) on immune function is controversial and NE has been shown to increase (Glac et al., 2006; Hellstrand, Hermodsson, & Strannegård, 1985; Tarr et al., 2012), decrease (Rosenne et al., 2014; Takamoto et al., 1991; Whalen & Bankhurst, 1990), or have no effect (Gotlieb et al., 2015) on NK cell immune function. This investigation sought to determine if NE suppressed NK cell function. NE treatment did not suppress NK cell lysis of tumor cells (NKCA), or suppress production of IFN gamma. With no effects seen in either NKCA or IFN gamma production for the 24 hr time period no epigenetic analyses were completed.

There are limitations to this investigation and chief among these is the *ex vivo* treatment of human PBMCs with Dex. It is unknown if the effects so observed *in vitro* would be achieved in subjects undergoing a psychologically stressful event. Further, we have explored a single histone epigenetic mark and a single immune effector molecule. However, H3K27me3 is a well characterized post-translational histone mark associated with repressed gene expression and with localization to heterochromatin. Likewise, we have explored only IFN gamma. However, IFN gamma is a hallmark cytokine produced by NK cells and is central to the innate and adaptive immune response. As such, it is likely that results obtained with this epigenetic mark and this cytokine are generalizable to overall immune function and to the effects of Dex on the chromatin organization of NK cells.

In conclusion, Dex was demonstrated to alter H3K27me3 CO and this alteration directly related to the capacity of NK cells to carry out immune function. Alterations in chromatin organization, as a downstream and more proximal indicator of immune function, may be an effective means by which to identify those at risk for GC induced immune dysregulation.

BIBLIOGRAPHY

- Abraham, S. M., Lawrence, T., Kleiman, A., Warden, P., Medghalchi, M., Tuckermann, J., . . . Clark, A. R. (2006). Antiinflammatory effects of dexamethasone are partly dependent on induction of dual specificity phosphatase 1. *J Exp Med*, 203(8), 1883-1889. doi:10.1084/jem.20060336
- Akhtar, A., & Gasser, S. M. (2007). The nuclear envelope and transcriptional control. *Nat Rev Genet*, 8(7), 507-517. doi:10.1038/nrg2122
- Almawi, W. Y., & Melemedjian, O. K. (2002). Negative regulation of nuclear factor-kappaB activation and function by glucocorticoids. *J Mol Endocrinol*, 28(2), 69-78.
- Amendola, M., & van Steensel, B. (2014). Mechanisms and dynamics of nuclear lamina-genome interactions. *Curr Opin Cell Biol*, 28, 61-68. doi:10.1016/j.ceb.2014.03.003
- Andrulis, E. D., Neiman, A. M., Zappulla, D. C., & Sternglanz, R. (1998). Perinuclear localization of chromatin facilitates transcriptional silencing. *Nature*, 394(6693), 592-595. doi:10.1038/29100
- Arib, G., & Akhtar, A. (2011). Multiple facets of nuclear periphery in gene expression control. *Curr Opin Cell Biol*, 23(3), 346-353. doi:10.1016/j.ceb.2010.12.005
- Ayroldi, E., Cannarile, L., Migliorati, G., Nocentini, G., Delfino, D. V., & Riccardi, C. (2012). Mechanisms of the anti-inflammatory effects of glucocorticoids: genomic and nongenomic interference with MAPK signaling pathways. *FASEB J*, 26(12), 4805-4820. doi:10.1096/fj.12-216382
- Barnes, P. J. (2006). Corticosteroid effects on cell signalling. *Eur Respir J*, 27(2), 413-426. doi:10.1183/09031936.06.00125404
- Barnes, P. J. (2010). Mechanisms and resistance in glucocorticoid control of inflammation. *J Steroid Biochem Mol Biol*, 120(2-3), 76-85. doi:10.1016/j.jsbmb.2010.02.018
- Beck, I. M., Vanden Berghe, W., Vermeulen, L., Yamamoto, K. R., Haegeman, G., & De Bosscher, K. (2009). Crosstalk in inflammation: the interplay of glucocorticoid receptor-based mechanisms and kinases and phosphatases. *Endocr Rev*, 30(7), 830-882. doi:10.1210/er.2009-0013

- Belmont, A. S., Zhai, Y., & Thilenius, A. (1993). Lamin B distribution and association with peripheral chromatin revealed by optical sectioning and electron microscopy tomography. *J Cell Biol*, *123*(6 Pt 2), 1671-1685.
- Bernardini, R., Chiarenza, A., Kamilaris, T. C., Renaud, N., Lempereur, L., Demitrack, M., . . . Chrousos, G. P. (1994). In vivo and in vitro effects of arginine-vasopressin receptor antagonists on the hypothalamic-pituitary-adrenal axis in the rat. *Neuroendocrinology*, *60*(5), 503-508.
- Bhattacharyya, S., Zhao, Y., Kay, T. W., & Muglia, L. J. (2011). Glucocorticoids target suppressor of cytokine signaling 1 (SOCS1) and type 1 interferons to regulate Toll-like receptor-induced STAT1 activation. *Proc Natl Acad Sci U S A*, *108*(23), 9554-9559. doi:10.1073/pnas.1017296108
- Biddie, S. C. (2011). Chromatin architecture and the regulation of nuclear receptor inducible transcription. *J Neuroendocrinol*, *23*(1), 94-106. doi:10.1111/j.1365-2826.2010.02079.x
- Blobel, G. (1985). Gene gating: a hypothesis. *Proc Natl Acad Sci U S A*, *82*(24), 8527-8529.
- Boumpas, D. T., Chrousos, G. P., Wilder, R. L., Cupps, T. R., & Balow, J. E. (1993). Glucocorticoid therapy for immune-mediated diseases: Basic and clinical correlates. *Annals of Internal Medicine*, *119*(12), 1198-1208. doi:10.7326/0003-4819-119-12-199312150-00007
- Bracken, A. P., Kleine-Kohlbrecher, D., Dietrich, N., Pasini, D., Gargiulo, G., Beekman, C., . . . Helin, K. (2007). The Polycomb group proteins bind throughout the INK4A-ARF locus and are disassociated in senescent cells. *Genes Dev*, *21*(5), 525-530. doi:10.1101/gad.415507
- Brickner, D. G., Ahmed, S., Meldi, L., Thompson, A., Light, W., Young, M., . . . Brickner, J. H. (2012). Transcription factor binding to a DNA zip code controls interchromosomal clustering at the nuclear periphery. *Dev Cell*, *22*(6), 1234-1246. doi:10.1016/j.devcel.2012.03.012
- Bush, K. A., Krukowski, K., Eddy, J. L., Janusek, L. W., & Mathews, H. L. (2012). Glucocorticoid receptor mediated suppression of natural killer cell activity: identification of associated deacetylase and corepressor molecules. *Cell Immunol*, *275*(1-2), 80-89. doi:10.1016/j.cellimm.2012.02.014
- Casolari, J. M., Brown, C. R., Komili, S., West, J., Hieronymus, H., & Silver, P. A. (2004). Genome-wide localization of the nuclear transport machinery couples transcriptional status and nuclear organization. *Cell*, *117*(4), 427-439.
- Connor, T. J., Brewer, C., Kelly, J. P., & Harkin, A. (2005). Acute stress suppresses pro-inflammatory cytokines TNF-alpha and IL-1 beta independent of a catecholamine-driven

- increase in IL-10 production. *J Neuroimmunol*, 159(1-2), 119-128.
doi:10.1016/j.jneuroim.2004.10.016
- Connor, T. J., Kelly, J. P., & Leonard, B. E. (1997). Forced swim test-induced neurochemical endocrine, and immune changes in the rat. *Pharmacol Biochem Behav*, 58(4), 961-967.
- Cooper, M. A., Fehniger, T. A., Turner, S. C., Chen, K. S., Ghaheri, B. A., Ghayur, T., . . . Caligiuri, M. A. (2001). Human natural killer cells: a unique innate immunoregulatory role for the CD56(bright) subset. *Blood*, 97(10), 3146-3151.
- Cosgrove, M. S., & Wolberger, C. (2005). How does the histone code work? *Biochem Cell Biol*, 83(4), 468-476. doi:10.1139/o05-137
- Cox, W. I., Holbrook, N. J., & Friedman, H. (1983). Mechanism of glucocorticoid action on murine natural killer cell activity. *J Natl Cancer Inst*, 71(5), 973-981.
- Cremer, M., Zinner, R., Stein, S., Albiez, H., Wagler, B., Cremer, C., & Cremer, T. (2004). Three dimensional analysis of histone methylation patterns in normal and tumor cell nuclei. *Eur J Histochem*, 48(1), 15-28.
- Curtin, N. M., Boyle, N. T., Mills, K. H., & Connor, T. J. (2009). Psychological stress suppresses innate IFN-gamma production via glucocorticoid receptor activation: reversal by the anxiolytic chlordiazepoxide. *Brain Behav Immun*, 23(4), 535-547.
doi:10.1016/j.bbi.2009.02.003
- Curtin, N. M., Mills, K. H., & Connor, T. J. (2009). Psychological stress increases expression of IL-10 and its homolog IL-19 via beta-adrenoceptor activation: reversal by the anxiolytic chlordiazepoxide. *Brain Behav Immun*, 23(3), 371-379. doi:10.1016/j.bbi.2008.12.010
- D'Adamio, F., Zollo, O., Moraca, R., Ayroldi, E., Bruscoli, S., Bartoli, A., . . . Riccardi, C. (1997). A new dexamethasone-induced gene of the leucine zipper family protects T lymphocytes from TCR/CD3-activated cell death. *Immunity*, 7(6), 803-812.
- De Bosscher, K., Vanden Berghe, W., & Haegeman, G. (2000). Mechanisms of anti-inflammatory action and of immunosuppression by glucocorticoids: negative interference of activated glucocorticoid receptor with transcription factors. *J Neuroimmunol*, 109(1), 16-22.
- De Bosscher, K., Vanden Berghe, W., Vermeulen, L., Plaisance, S., Boone, E., & Haegeman, G. (2000). Glucocorticoids repress NF-kappaB-driven genes by disturbing the interaction of p65 with the basal transcription machinery, irrespective of coactivator levels in the cell. *Proc Natl Acad Sci U S A*, 97(8), 3919-3924.
- Dhabhar, F. S., & McEwen, B. S. (1997). Acute Stress Enhances while Chronic Stress Suppresses Cell-Mediated Immunity in Vivo: A Potential Role for Leukocyte Trafficking.

Brain, Behavior, and Immunity, 11(4), 286-306.
doi:<https://doi.org/10.1006/brbi.1997.0508>

- Dhabhar, F. S., Miller, A. H., McEwen, B. S., & Spencer, R. L. (1995). Effects of stress on immune cell distribution. Dynamics and hormonal mechanisms. *J Immunol*, 154(10), 5511-5527.
- Dhabhar, F. S., Miller, A. H., Stein, M., McEwen, B. S., & Spencer, R. L. (1994). Diurnal and acute stress-induced changes in distribution of peripheral blood leukocyte subpopulations. *Brain Behav Immun*, 8(1), 66-79. doi:10.1006/brbi.1994.1006
- Dixon, J. R., Selvaraj, S., Yue, F., Kim, A., Li, Y., Shen, Y., . . . Ren, B. (2012). Topological domains in mammalian genomes identified by analysis of chromatin interactions. *Nature*, 485(7398), 376-380. doi:10.1038/nature11082
- Eddy, J. L., Krukowski, K., Janusek, L., & Mathews, H. L. (2014). Glucocorticoids regulate natural killer cell function epigenetically. *Cell Immunol*, 290(1), 120-130. doi:10.1016/j.cellimm.2014.05.013
- Egecioglu, D., & Brickner, J. H. (2011). Gene positioning and expression. *Curr Opin Cell Biol*, 23(3), 338-345. doi:10.1016/j.ceb.2011.01.001
- Elenkov, I. J., Wilder, R. L., Chrousos, G. P., & Vizi, E. S. (2000). The sympathetic nerve--an integrative interface between two supersystems: the brain and the immune system. *Pharmacol Rev*, 52(4), 595-638.
- Falkenstein, E., Tillmann, H. C., Christ, M., Feuring, M., & Wehling, M. (2000). Multiple actions of steroid hormones--a focus on rapid, nongenomic effects. *Pharmacol Rev*, 52(4), 513-556.
- Filipe-Santos, O., Bustamante, J., Chapgier, A., Vogt, G., de Beaucoudrey, L., Feinberg, J., . . . Casanova, J. L. (2006). Inborn errors of IL-12/23- and IFN-gamma-mediated immunity: molecular, cellular, and clinical features. *Semin Immunol*, 18(6), 347-361. doi:10.1016/j.smim.2006.07.010
- Flammer, J. R., & Rogatsky, I. (2011). Minireview: Glucocorticoids in autoimmunity: unexpected targets and mechanisms. *Mol Endocrinol*, 25(7), 1075-1086. doi:10.1210/me.2011-0068
- Galon, J., Franchimont, D., Hiroi, N., Frey, G., Boettner, A., Ehrhart-Bornstein, M., . . . Bornstein, S. R. (2002). Gene profiling reveals unknown enhancing and suppressive actions of glucocorticoids on immune cells. *FASEB J*, 16(1), 61-71. doi:10.1096/fj.01-0245com

- Gatti, G., Cavallo, R., Sartori, M. L., Marinone, C., & Angeli, A. (1986). Cortisol at physiological concentrations and prostaglandin E2 are additive inhibitors of human natural killer cell activity. *Immunopharmacology*, *11*(2), 119-128.
- Gibcus, J. H., & Dekker, J. (2013). The hierarchy of the 3D genome. *Mol Cell*, *49*(5), 773-782. doi:10.1016/j.molcel.2013.02.011
- Glac, W., Borman, A., Badtke, P., Stojek, W., Orlikowska, A., & Tokarski, J. (2006). Amphetamine enhances natural killer cytotoxic activity via beta-adrenergic mechanism. *J Physiol Pharmacol*, *57 Suppl 11*, 125-132.
- Glaser, R., & Kiecolt-Glaser, J. K. (2005). Stress-induced immune dysfunction: implications for health. *Nat Rev Immunol*, *5*(3), 243-251. doi:10.1038/nri1571
- Gotlieb, N., Rosenne, E., Matzner, P., Shaashua, L., Sorski, L., & Ben-Eliyahu, S. (2015). The misleading nature of in vitro and ex vivo findings in studying the impact of stress hormones on NK cell cytotoxicity. *Brain Behav Immun*, *45*, 277-286. doi:10.1016/j.bbi.2014.12.020
- Goujon, E., Parnet, P., Laye, S., Combe, C., Kelley, K. W., & Dantzer, R. (1995). Stress downregulates lipopolysaccharide-induced expression of proinflammatory cytokines in the spleen, pituitary, and brain of mice. *Brain Behav Immun*, *9*(4), 292-303. doi:10.1006/brbi.1995.1028
- Green, E. M., Jiang, Y., Joyner, R., & Weis, K. (2012). A negative feedback loop at the nuclear periphery regulates GAL gene expression. *Mol Biol Cell*, *23*(7), 1367-1375. doi:10.1091/mbc.E11-06-0547
- Grewal, S. I., & Moazed, D. (2003). Heterochromatin and epigenetic control of gene expression. *Science*, *301*(5634), 798-802. doi:10.1126/science.1086887
- Groeneweg, F. L., Karst, H., de Kloet, E. R., & Joëls, M. (2011). Rapid non-genomic effects of corticosteroids and their role in the central stress response. *J Endocrinol*, *209*(2), 153-167. doi:10.1530/JOE-10-0472
- Guelen, L., Pagie, L., Brasset, E., Meuleman, W., Faza, M. B., Talhout, W., . . . van Steensel, B. (2008). Domain organization of human chromosomes revealed by mapping of nuclear lamina interactions. *Nature*, *453*(7197), 948-951. doi:10.1038/nature06947
- Haberland, M., Montgomery, R. L., & Olson, E. N. (2009). The many roles of histone deacetylases in development and physiology: implications for disease and therapy. *Nat Rev Genet*, *10*(1), 32-42. doi:10.1038/nrg2485
- Haraguchi, S., Good, R. A., & Day, N. K. (1995). Immunosuppressive retroviral peptides: cAMP and cytokine patterns. *Immunol Today*, *16*(12), 595-603. doi:10.1016/0167-5699(95)80083-2

- Haraguchi, S., Good, R. A., James-Yarish, M., Cianciolo, G. J., & Day, N. K. (1995a). Differential modulation of Th1- and Th2-related cytokine mRNA expression by a synthetic peptide homologous to a conserved domain within retroviral envelope protein. *Proc Natl Acad Sci U S A*, *92*(8), 3611-3615.
- Haraguchi, S., Good, R. A., James-Yarish, M., Cianciolo, G. J., & Day, N. K. (1995b). Induction of intracellular cAMP by a synthetic retroviral envelope peptide: a possible mechanism of immunopathogenesis in retroviral infections. *Proc Natl Acad Sci U S A*, *92*(12), 5568-5571.
- Hayashi, A., Yamauchi, N., Shibahara, J., Kimura, H., Morikawa, T., Ishikawa, S., . . . Fukayama, M. (2014). Concurrent activation of acetylation and tri-methylation of H3K27 in a subset of hepatocellular carcinoma with aggressive behavior. *PLoS ONE*, *9*(3): e91330.
- Hellstrand, K., Hermodsson, S., & Strannegård, O. (1985). Evidence for a beta-adrenoceptor-mediated regulation of human natural killer cells. *J Immunol*, *134*(6), 4095-4099.
- Hersey, P., Edwards, A., Honeyman, M., & McCarthy, W. H. (1979). Low natural-killer-cell activity in familial melanoma patients and their relatives. *Br J Cancer*, *40*(1), 113-122.
- Hosoi, T., Okuma, Y., & Nomura, Y. (2000). Electrical stimulation of afferent vagus nerve induces IL-1beta expression in the brain and activates HPA axis. *Am J Physiol Regul Integr Comp Physiol*, *279*(1), R141-147.
- Ikegami, K., & Lieb, J. D. (2013). Integral nuclear pore proteins bind to Pol III-transcribed genes and are required for Pol III transcript processing in *C. elegans*. *Mol Cell*, *51*(6), 840-849. doi:10.1016/j.molcel.2013.08.001
- Imai, K., Matsuyama, S., Miyake, S., Suga, K., & Nakachi, K. (2000). Natural cytotoxic activity of peripheral-blood lymphocytes and cancer incidence: an 11-year follow-up study of a general population. *Lancet*, *356*(9244), 1795-1799. doi:10.1016/S0140-6736(00)03231-1
- Irwin, M., Hauger, R., & Brown, M. (1992). Central corticotropin-releasing hormone activates the sympathetic nervous system and reduces immune function: increased responsivity of the aged rat. *Endocrinology*, *131*(3), 1047-1053. doi:10.1210/endo.131.3.1505449
- John, S., Sabo, P. J., Thurman, R. E., Sung, M. H., Biddie, S. C., Johnson, T. A., . . . Stamatoyannopoulos, J. A. (2011). Chromatin accessibility pre-determines glucocorticoid receptor binding patterns. *Nat Genet*, *43*(3), 264-268. doi:10.1038/ng.759
- Karin, M. (1998). New twists in gene regulation by glucocorticoid receptor: is DNA binding dispensable? *Cell*, *93*(4), 487-490.

- Kawakami, K., Nakamura, A., Ishigami, A., Goto, S., & Takahashi, R. (2009). Age-related difference of site-specific histone modifications in rat liver. *Biogerontology*, *10*(4), 415-421. doi:10.1007/s10522-008-9176-0
- Khan, M. M., Sansoni, P., Silverman, E. D., Engleman, E. G., & Melmon, K. L. (1986). Beta-adrenergic receptors on human suppressor, helper, and cytolytic lymphocytes. *Biochem Pharmacol*, *35*(7), 1137-1142.
- Kim, J. S., & Shukla, S. D. (2006). Acute in vivo effect of ethanol (binge drinking) on histone H3 modifications in rat tissues. *Alcohol Alcohol*, *41*(2), 126-132. doi:10.1093/alcalc/agh248
- Kitakaze, M., Hori, M., Sato, H., Takashima, S., Inoue, M., Kitabatake, A., & Kamada, T. (1991). Endogenous adenosine inhibits platelet aggregation during myocardial ischemia in dogs. *Circ Res*, *69*(5), 1402-1408.
- Kouzarides, T. (2007). Chromatin modifications and their function. *Cell*, *128*(4), 693-705. doi:10.1016/j.cell.2007.02.005
- Krukowski, K., Eddy, J., Kosik, K. L., Konley, T., Janusek, L. W., & Mathews, H. L. (2011). Glucocorticoid dysregulation of natural killer cell function through epigenetic modification. *Brain Behav Immun*, *25*(2), 239-249. doi:10.1016/j.bbi.2010.07.244
- Krull, S., Dörries, J., Boysen, B., Reidenbach, S., Magnius, L., Norder, H., . . . Cordes, V. C. (2010). Protein Tpr is required for establishing nuclear pore-associated zones of heterochromatin exclusion. *EMBO J*, *29*(10), 1659-1673. doi:10.1038/emboj.2010.54
- Krzewski, K., Gil-Krzewska, A., Nguyen, V., Peruzzi, G., & Coligan, J. E. (2013). LAMP1/CD107a is required for efficient perforin delivery to lytic granules and NK-cell cytotoxicity. *Blood*, *121*(23), 4672-4683. doi:10.1182/blood-2012-08-453738
- Kusnecov, A. W., & Rabin, B. S. (1994). Stressor-induced alterations of immune function: mechanisms and issues. *Int Arch Allergy Immunol*, *105*(2), 107-121.
- Kuznetsova, T., Wang, S. Y., Rao, N. A., Mandoli, A., Martens, J. H., Rother, N., . . . Stunnenberg, H. G. (2015). Glucocorticoid receptor and nuclear factor kappa-b affect three-dimensional chromatin organization. *Genome Biol*, *16*, 264. doi:10.1186/s13059-015-0832-9
- Laugero, K. D., & Moberg, G. P. (2000). Effects of acute behavioral stress and LPS-induced cytokine release on growth and energetics in mice. *Physiol Behav*, *68*(3), 415-422.
- Li, H. B., Ohno, K., Gui, H., & Pirrotta, V. (2013). Insulators target active genes to transcription factories and polycomb-repressed genes to polycomb bodies. *PLoS Genet*, *9*(4), e1003436. doi:10.1371/journal.pgen.1003436

- Li, X., Wong, J., Tsai, S. Y., Tsai, M. J., & O'Malley, B. W. (2003). Progesterone and glucocorticoid receptors recruit distinct coactivator complexes and promote distinct patterns of local chromatin modification. *Mol Cell Biol*, *23*(11), 3763-3773.
- Lieberman-Aiden, E., van Berkum, N. L., Williams, L., Imakaev, M., Ragoczy, T., Telling, A., . . . Dekker, J. (2009). Comprehensive mapping of long-range interactions reveals folding principles of the human genome. *Science*, *326*(5950), 289-293.
- Light, W. H., Brickner, D. G., Brand, V. R., & Brickner, J. H. (2010). Interaction of a DNA zip code with the nuclear pore complex promotes H2A.Z incorporation and INO1 transcriptional memory. *Mol Cell*, *40*(1), 112-125. doi:10.1016/j.molcel.2010.09.007
- Löwenberg, M., Verhaar, A. P., van den Brink, G. R., & Hommes, D. W. (2007). Glucocorticoid signaling: a nongenomic mechanism for T-cell immunosuppression. *Trends Mol Med*, *13*(4), 158-163. doi:10.1016/j.molmed.2007.02.001
- Ma, S., & Morilak, D. A. (2005). Norepinephrine release in medial amygdala facilitates activation of the hypothalamic-pituitary-adrenal axis in response to acute immobilisation stress. *J Neuroendocrinol*, *17*(1), 22-28. doi:10.1111/j.1365-2826.2005.01279.x
- Madden, K. S., Felten, S. Y., Felten, D. L., & Bellinger, D. L. (1995). Sympathetic nervous system--immune system interactions in young and old Fischer 344 rats. *Ann N Y Acad Sci*, *771*, 523-534.
- Madden, K. S., Sanders, V. M., & Felten, D. L. (1995). Catecholamine influences and sympathetic neural modulation of immune responsiveness. *Annu Rev Pharmacol Toxicol*, *35*, 417-448. doi:10.1146/annurev.pa.35.040195.002221
- Maisel, A. S., Harris, T., Rearden, C. A., & Michel, M. C. (1990). Beta-adrenergic receptors in lymphocyte subsets after exercise. Alterations in normal individuals and patients with congestive heart failure. *Circulation*, *82*(6), 2003-2010.
- Margueron, R., Justin, N., Ohno, K., Sharpe, M. L., Son, J., Drury, W. J., . . . Gambin, S. J. (2009). Role of the polycomb protein EED in the propagation of repressive histone marks. *Nature*, *461*(7265), 762-767. doi:10.1038/nature08398
- Margueron, R., & Reinberg, D. (2011). The Polycomb complex PRC2 and its mark in life. *Nature*, *469*(7330), 343-349. doi:10.1038/nature09784
- Martin, C., & Zhang, Y. (2005). The diverse functions of histone lysine methylation. *Nat Rev Mol Cell Biol*, *6*(11), 838-849. doi:10.1038/nrm1761
- Mathews, H. L., Konley, T., Kosik, K. L., Krukowski, K., Eddy, J., Albuquerque, K., & Janusek, L. W. (2011). Epigenetic patterns associated with the immune dysregulation that accompanies psychosocial distress. *Brain Behav Immun*, *25*(5), 830-839. doi:10.1016/j.bbi.2010.12.002

- McNally, J. G., Müller, W. G., Walker, D., Wolford, R., & Hager, G. L. (2000). The glucocorticoid receptor: rapid exchange with regulatory sites in living cells. *Science*, 287(5456), 1262-1265.
- Meltzer, J. C., MacNeil, B. J., Sanders, V., Pylypas, S., Jansen, A. H., Greenberg, A. H., & Nance, D. M. (2004). Stress-induced suppression of in vivo splenic cytokine production in the rat by neural and hormonal mechanisms. *Brain Behav Immun*, 18(3), 262-273. doi:10.1016/j.bbi.2003.09.003
- Merkenschlager, M., & Odom, D. T. (2013). CTCF and cohesin: linking gene regulatory elements with their targets. *Cell*, 152(6), 1285-1297. doi:10.1016/j.cell.2013.02.029
- Misteli, T. (2007). Beyond the sequence: cellular organization of genome function. *Cell*, 128(4), 787-800. doi:10.1016/j.cell.2007.01.028
- Morvan, M. G., & Lanier, L. L. (2016). NK cells and cancer: you can teach innate cells new tricks. *Nat Rev Cancer*, 16(1), 7-19. doi:10.1038/nrc.2015.5
- Nakajima, T., Mizushima, N., Nakamura, J., & Kanai, K. (1986). Surface markers of NK cells in peripheral blood of patients with cirrhosis and hepatocellular carcinoma. *Immunol Lett*, 13(1-2), 7-10.
- Nicolaidis, N. C., Galata, Z., Kino, T., Chrousos, G. P., & Charmandari, E. (2010). The human glucocorticoid receptor: molecular basis of biologic function. *Steroids*, 75(1), 1-12. doi:10.1016/j.steroids.2009.09.002
- Nielsen, S. J., Schneider, R., Bauer, U. M., Bannister, A. J., Morrison, A., O'Carroll, D., . . . Kouzarides, T. (2001). Rb targets histone H3 methylation and HP1 to promoters. *Nature*, 412(6846), 561-565. doi:10.1038/35087620
- O'Sullivan, T., Saddawi-Konefka, R., Vermi, W., Koebel, C. M., Arthur, C., White, J. M., . . . Bui, J. D. (2012). Cancer immunoediting by the innate immune system in the absence of adaptive immunity. *J Exp Med*, 209(10), 1869-1882. doi:10.1084/jem.20112738
- Oakley, R. H., & Cidlowski, J. A. (2013). The biology of the glucocorticoid receptor: new signaling mechanisms in health and disease. *J Allergy Clin Immunol*, 132(5), 1033-1044. doi:10.1016/j.jaci.2013.09.007
- Olnes, M. J., Kotliarov, Y., Biancotto, A., Cheung, F., Chen, J., Shi, R., . . . Consortium, C. (2016). Effects of Systemically Administered Hydrocortisone on the Human Immunome. *Sci Rep*, 6, 23002. doi:10.1038/srep23002
- Orange, J. S. (2006). Human natural killer cell deficiencies. *Curr Opin Allergy Clin Immunol*, 6(6), 399-409. doi:10.1097/ACI.0b013e3280106b65

- Orange, J. S. (2013). Natural killer cell deficiency. *J Allergy Clin Immunol*, *132*(3), 515-525; quiz 526. doi:10.1016/j.jaci.2013.07.020
- Osborne, C. S., Chakalova, L., Brown, K. E., Carter, D., Horton, A., Debrand, E., . . . Fraser, P. (2004). Active genes dynamically colocalize to shared sites of ongoing transcription. *Nat Genet*, *36*(10), 1065-1071. doi:10.1038/ng1423
- Panina-Bordignon, P., Mazzeo, D., Lucia, P. D., D'Ambrosio, D., Lang, R., Fabbri, L., . . . Sinigaglia, F. (1997). Beta2-agonists prevent Th1 development by selective inhibition of interleukin 12. *J Clin Invest*, *100*(6), 1513-1519. doi:10.1172/JCI119674
- Parry, G. C., & Mackman, N. (1997). Role of cyclic AMP response element-binding protein in cyclic AMP inhibition of NF-kappaB-mediated transcription. *J Immunol*, *159*(11), 5450-5456.
- Pascual-Garcia, P., & Capelson, M. (2014). Nuclear pores as versatile platforms for gene regulation. *Curr Opin Genet Dev*, *25*, 110-117. doi:10.1016/j.gde.2013.12.009
- Pross, H. F., & Lotzová, E. (1993). Role of natural killer cells in cancer. *Nat Immun*, *12*(4-5), 279-292.
- Rao, S. S., Huntley, M. H., Durand, N. C., Stamenova, E. K., Bochkov, I. D., Robinson, J. T., . . . Aiden, E. L. (2014). A 3D map of the human genome at kilobase resolution reveals principles of chromatin looping. *Cell*, *159*(7), 1665-1680. doi:10.1016/j.cell.2014.11.021
- Reddy, T. E., Pauli, F., Sprouse, R. O., Neff, N. F., Newberry, K. M., Garabedian, M. J., & Myers, R. M. (2009). Genomic determination of the glucocorticoid response reveals unexpected mechanisms of gene regulation. *Genome Res*, *19*(12), 2163-2171. doi:10.1101/gr.097022.109
- Reily, M. M., Pantoja, C., Hu, X., Chinenov, Y., & Rogatsky, I. (2006). The GRIP1:IRF3 interaction as a target for glucocorticoid receptor-mediated immunosuppression. *EMBO J*, *25*(1), 108-117. doi:10.1038/sj.emboj.7600919
- Rosenne, E., Sorski, L., Shaashua, L., Neeman, E., Matzner, P., Levi, B., & Ben-Eliyahu, S. (2014). In vivo suppression of NK cell cytotoxicity by stress and surgery: glucocorticoids have a minor role compared to catecholamines and prostaglandins. *Brain Behav Immun*, *37*, 207-219. doi:10.1016/j.bbi.2013.12.007
- Sadhu, M. J., Guan, Q., Li, F., Sales-Lee, J., Iavarone, A. T., Hammond, M. C., . . . Rine, J. (2013). Nutritional control of epigenetic processes in yeast and human cells. *Genetics*, *195*(3), 831-844. doi:10.1534/genetics.113.153981
- Sanders, V. M., Baker, R. A., Ramer-Quinn, D. S., Kasprovicz, D. J., Fuchs, B. A., & Street, N. E. (1997). Differential expression of the beta2-adrenergic receptor by Th1 and Th2

- clones: implications for cytokine production and B cell help. *J Immunol*, 158(9), 4200-4210.
- Schantz, S. P., Shillitoe, E. J., Brown, B., & Campbell, B. (1986). Natural killer cell activity and head and neck cancer: a clinical assessment. *J Natl Cancer Inst*, 77(4), 869-875.
- Schermelleh, L., Carlton, P. M., Haase, S., Shao, L., Winoto, L., Kner, P., . . . Sedat, J. W. (2008). Subdiffraction multicolor imaging of the nuclear periphery with 3D structured illumination microscopy. *Science*, 320(5881), 1332-1336. doi:10.1126/science.1156947
- Schmid, M., Arib, G., Laemmli, C., Nishikawa, J., Durussel, T., & Laemmli, U. K. (2006). Nup-PI: the nucleopore-promoter interaction of genes in yeast. *Mol Cell*, 21(3), 379-391. doi:10.1016/j.molcel.2005.12.012
- Schneider, R., & Grosschedl, R. (2007). Dynamics and interplay of nuclear architecture, genome organization, and gene expression. *Genes Dev*, 21(23), 3027-3043. doi:10.1101/gad.1604607
- Segerstrom, S. C., & Miller, G. E. (2004). Psychological stress and the human immune system: a meta-analytic study of 30 years of inquiry. *Psychol Bull*, 130(4), 601-630. doi:10.1037/0033-2909.130.4.601
- Shanks, N., Griffiths, J., Zalcman, S., Zacharko, R. M., & Anisman, H. (1990). Mouse strain differences in plasma corticosterone following uncontrollable footshock. *Pharmacol Biochem Behav*, 36(3), 515-519.
- Shakhar, G., Abudarham, N., Melamed, R., Schwartz, Y., Rosenne, E., & Ben-Eliyahu, S. (2007). Amelioration of operation-induced suppression of marginating pulmonary NK activity using poly IC: a potential approach to reduce postoperative metastasis. *Ann Surg Oncol*, 14(2), 841-852. doi:10.1245/s10434-006-9078-9
- Sheridan, J. F., Feng, N. G., Bonneau, R. H., Allen, C. M., Huneycutt, B. S., & Glaser, R. (1991). Restraint stress differentially affects anti-viral cellular and humoral immune responses in mice. *J Neuroimmunol*, 31(3), 245-255.
- Simon, J. A., & Kingston, R. E. (2009). Mechanisms of polycomb gene silencing: knowns and unknowns. *Nat Rev Mol Cell Biol*, 10(10), 697-708. doi:10.1038/nrm2763
- So, A. Y., Chaivorapol, C., Bolton, E. C., Li, H., & Yamamoto, K. R. (2007). Determinants of cell- and gene-specific transcriptional regulation by the glucocorticoid receptor. *PLoS Genet*, 3(6), e94. doi:10.1371/journal.pgen.0030094
- Spinner, M. A., Sanchez, L. A., Hsu, A. P., Shaw, P. A., Zerbe, C. S., Calvo, K. R., . . . Holland, S. M. (2014). GATA2 deficiency: a protean disorder of hematopoiesis, lymphatics, and immunity. *Blood*, 123(6), 809-821. doi:10.1182/blood-2013-07-515528

- Spivakov, M., & Fisher, A. G. (2007). Epigenetic signatures of stem-cell identity. *Nat Rev Genet*, 8(4), 263-271. doi:10.1038/nrg2046
- Stahn, C., & Buttgerit, F. (2008). Genomic and nongenomic effects of glucocorticoids. *Nat Clin Pract Rheumatol*, 4(10), 525-533. doi:10.1038/ncprheum0898
- Stahn, C., Löwenberg, M., Hommes, D. W., & Buttgerit, F. (2007). Molecular mechanisms of glucocorticoid action and selective glucocorticoid receptor agonists. *Mol Cell Endocrinol*, 275(1-2), 71-78. doi:10.1016/j.mce.2007.05.019
- Stetson, D. B., Mohrs, M., Reinhardt, R. L., Baron, J. L., Wang, Z. E., Gapin, L., . . . Locksley, R. M. (2003). Constitutive cytokine mRNAs mark natural killer (NK) and NK T cells poised for rapid effector function. *J Exp Med*, 198(7), 1069-1076. doi:10.1084/jem.20030630
- Strayer, D. R., Carter, W. A., & Brodsky, I. (1986). Familial occurrence of breast cancer is associated with reduced natural killer cytotoxicity. *Breast Cancer Res Treat*, 7(3), 187-192.
- Sundar, I. K., Nevid, M. Z., Friedman, A. E., & Rahman, I. (2014). Cigarette smoke induces distinct histone modifications in lung cells: implications for the pathogenesis of COPD and lung cancer. *J Proteome Res*, 13(2), 982-996. doi:10.1021/pr400998n
- Surjit, M., Ganti, K. P., Mukherji, A., Ye, T., Hua, G., Metzger, D., . . . Chambon, P. (2011). Widespread negative response elements mediate direct repression by agonist-liganded glucocorticoid receptor. *Cell*, 145(2), 224-241. doi:10.1016/j.cell.2011.03.027
- Taddei, A., Van Houwe, G., Hediger, F., Kalck, V., Cubizolles, F., Schober, H., & Gasser, S. M. (2006). Nuclear pore association confers optimal expression levels for an inducible yeast gene. *Nature*, 441(7094), 774-778. doi:10.1038/nature04845
- Takamoto, T., Hori, Y., Koga, Y., Toshima, H., Hara, A., & Yokoyama, M. M. (1991). Norepinephrine inhibits human natural killer cell activity in vitro. *Int J Neurosci*, 58(1-2), 127-131.
- Tarr, A. J., Powell, N. D., Reader, B. F., Bhave, N. S., Roloson, A. L., Carson, W. E., & Sheridan, J. F. (2012). β -Adrenergic receptor mediated increases in activation and function of natural killer cells following repeated social disruption. *Brain Behav Immun*, 26(8), 1226-1238. doi:10.1016/j.bbi.2012.07.002
- Tie, F., Furuyama, T., Prasad-Sinha, J., Jane, E., & Harte, P. J. (2001). The Drosophila Polycomb Group proteins ESC and E(Z) are present in a complex containing the histone-binding protein p55 and the histone deacetylase RPD3. *Development*, 128(2), 275-286.

- Torpy, D. J., & Ho, J. T. (2007). Corticosteroid-binding globulin gene polymorphisms: clinical implications and links to idiopathic chronic fatigue disorders. *Clin Endocrinol (Oxf)*, *67*(2), 161-167. doi:10.1111/j.1365-2265.2007.02890.x
- Uhlenhaut, N. H., Barish, G. D., Yu, R. T., Downes, M., Karunasiri, M., Liddle, C., . . . Evans, R. M. (2013). Insights into negative regulation by the glucocorticoid receptor from genome-wide profiling of inflammatory cistromes. *Mol Cell*, *49*(1), 158-171. doi:10.1016/j.molcel.2012.10.013
- Van de Vosse, D. W., Wan, Y., Lapetina, D. L., Chen, W. M., Chiang, J. H., Aitchison, J. D., & Wozniak, R. W. (2013). A role for the nucleoporin Nup170p in chromatin structure and gene silencing. *Cell*, *152*(5), 969-983. doi:10.1016/j.cell.2013.01.049
- van der Vlag, J., & Otte, A. P. (1999). Transcriptional repression mediated by the human polycomb-group protein EED involves histone deacetylation. *Nat Genet*, *23*(4), 474-478. doi:10.1038/70602
- Van Laethem, F., Liang, X., Andris, F., Urbain, J., Vandenbranden, M., Ruyschaert, J. M., . . . Leo, O. (2003). Glucocorticoids alter the lipid and protein composition of membrane rafts of a murine T cell hybridoma. *J Immunol*, *170*(6), 2932-2939.
- Vieira, P. L., Kaliński, P., Wierenga, E. A., Kapsenberg, M. L., & de Jong, E. C. (1998). Glucocorticoids inhibit bioactive IL-12p70 production by in vitro-generated human dendritic cells without affecting their T cell stimulatory potential. *J Immunol*, *161*(10), 5245-5251.
- Visser, J., van Boxel-Dezaire, A., Methorst, D., Brunt, T., de Kloet, E. R., & Nagelkerken, L. (1998). Differential regulation of interleukin-10 (IL-10) and IL-12 by glucocorticoids in vitro. *Blood*, *91*(11), 4255-4264.
- Vivier, E., Raulet, D. H., Moretta, A., Caligiuri, M. A., Zitvogel, L., Lanier, L. L., . . . Ugolini, S. (2011). Innate or adaptive immunity? The example of natural killer cells. *Science*, *331*(6013), 44-49. doi:10.1126/science.1198687
- Vivier, E., Tomasello, E., Baratin, M., Walzer, T., & Ugolini, S. (2008). Functions of natural killer cells. *Nat Immunol*, *9*(5), 503-510. doi:10.1038/ni1582
- Vockley, C. M., D'Ippolito, A. M., McDowell, I. C., Majoros, W. H., Safi, A., Song, L., . . . Reddy, T. E. (2016). Direct GR Binding Sites Potentiate Clusters of TF Binding across the Human Genome. *Cell*, *166*(5), 1269-1281.e1219. doi:10.1016/j.cell.2016.07.049
- Voss, T. C., Schiltz, R. L., Sung, M. H., Yen, P. M., Stamatoyannopoulos, J. A., Biddie, S. C., . . . Hager, G. L. (2011). Dynamic exchange at regulatory elements during chromatin remodeling underlies assisted loading mechanism. *Cell*, *146*(4), 544-554. doi:10.1016/j.cell.2011.07.006

- Wang, J. C., Derynck, M. K., Nonaka, D. F., Khodabakhsh, D. B., Haqq, C., & Yamamoto, K. R. (2004). Chromatin immunoprecipitation (ChIP) scanning identifies primary glucocorticoid receptor target genes. *Proc Natl Acad Sci U S A*, *101*(44), 15603-15608. doi:10.1073/pnas.0407008101
- Wang, S., Su, J. H., Beliveau, B. J., Bintu, B., Moffitt, J. R., Wu, C. T., & Zhuang, X. (2016). Spatial organization of chromatin domains and compartments in single chromosomes. *Science*, *353*(6299), 598-602. doi:10.1126/science.aaf8084
- Whalen, M. M., & Bankhurst, A. D. (1990). Effects of beta-adrenergic receptor activation, cholera toxin and forskolin on human natural killer cell function. *Biochem J*, *272*(2), 327-331.
- Whirledge, S., Xu, X., & Cidlowski, J. A. (2013). Global gene expression analysis in human uterine epithelial cells defines new targets of glucocorticoid and estradiol antagonism. *Biol Reprod*, *89*(3), 66. doi:10.1095/biolreprod.113.111054
- Whitnall, M. H. (1993). Regulation of the hypothalamic corticotropin-releasing hormone neurosecretory system. *Prog Neurobiol*, *40*(5), 573-629.
- Wilckens, T., & De Rijk, R. (1997). Glucocorticoids and immune function: unknown dimensions and new frontiers. *Immunol Today*, *18*(9), 418-424.
- Witek-Janusek, L., Albuquerque, K., Chroniak, K. R., Chroniak, C., Durazo-Arvizu, R., & Mathews, H. L. (2008). Effect of mindfulness based stress reduction on immune function, quality of life and coping in women newly diagnosed with early stage breast cancer. *Brain Behav Immun*, *22*(6), 969-981. doi:10.1016/j.bbi.2008.01.012
- Witek-Janusek, L., Gabram, S., & Mathews, H. L. (2007). Psychologic stress, reduced NK cell activity, and cytokine dysregulation in women experiencing diagnostic breast biopsy. *Psychoneuroendocrinology*, *32*(1), 22-35. doi:10.1016/j.psyneuen.2006.09.011
- Williams, R. R., Azuara, V., Perry, P., Sauer, S., Dvorkina, M., Jørgensen, H., . . . Fisher, A. G. (2006). Neural induction promotes large-scale chromatin reorganisation of the Mash1 locus. *J Cell Sci*, *119*(Pt 1), 132-140. doi:10.1242/jcs.02727
- Yamagata, S., Tomita, K., Sano, H., Itoh, Y., Fukai, Y., Okimoto, N., . . . Tohda, Y. (2012). Non-genomic inhibitory effect of glucocorticoids on activated peripheral blood basophils through suppression of lipid raft formation. *Clin Exp Immunol*, *170*(1), 86-93. doi:10.1111/j.1365-2249.2012.04636.x
- Yang, S. R., Valvo, S., Yao, H., Kode, A., Rajendrasozhan, S., Edirisinghe, I., . . . Rahman, I. (2008). IKK alpha causes chromatin modification on pro-inflammatory genes by cigarette smoke in mouse lung. *Am J Respir Cell Mol Biol*, *38*(6), 689-698. doi:10.1165/rcmb.2007-0379OC

- Zhao, Q., Wang, X., Nelin, L. D., Yao, Y., Matta, R., Manson, M. E., . . . Liu, Y. (2006). MAP kinase phosphatase 1 controls innate immune responses and suppresses endotoxic shock. *J Exp Med*, *203*(1), 131-140. doi:10.1084/jem.20051794
- Zhou, J., Zhang, J., Lichtenheld, M. G., & Meadows, G. G. (2002). A role for NF-kappa B activation in perforin expression of NK cells upon IL-2 receptor signaling. *J Immunol*, *169*(3), 1319-1325.
- Zink, D., Fischer, A. H., & Nickerson, J. A. (2004). Nuclear structure in cancer cells. *Nat Rev Cancer*, *4*(9), 677-687. doi:10.1038/nrc1430

VITA

The author, Michael S. Misale, was born in Chicago, IL on May 15, 1985 to Ricky and Linda Misale. He attended Carthage College in Kenosha, Wisconsin where he earned a Bachelor's of Arts, *cum laude*, in Biology in May 2007. After graduation Michael worked as a research technologist in the lab of Allen Cowley at the Medical College of Wisconsin in Wauwatosa, Wisconsin and performed studies to elucidate the genetic mechanisms underlying hypertension in rat model systems. In July of 2009, Michael then worked as a research technologist for Karen Visick at Loyola University Chicago studying the transcriptional regulation of a gene locus required for a squid-bacteria symbiosis. It was the mentorship of Allen Cowley and Karen Visick that urged Michael to pursue a graduate degree. In August 2010, Michael matriculated into the Loyola University Chicago Stritch School of Microbiology and Immunology Graduate Program and joined the lab of Herbert Mathews.

Michael's thesis work explored the impact of glucocorticoids on global H3K27me3 chromatin organization and the relationship of H3K27me3 chromatin organization to interferon gamma production in natural killer cells. After completion of his graduate studies, Michael will be seeking employment studying cancer immunotherapy and teaching biology courses.

